치의과학박사 학위논문

Mechanism of rescuing *Runx2* haplodeficiency-induced cleidocranial dysplasia by histone deacetylase inhibition

Runx2$^{+/-}$ 두개쇄골이형성증 마우스에서
히스톤 탈아세틸화효소 억제에 의한 뼈 이상 회복 기전 연구

2017년 8월

서울대학교 대학원

치의과학과 분자유전학 전공

배 한 솔

Mechanism of rescuing *Runx2* haplodeficiency-induced cleidocranial dysplasia by histone deacetylase inhibition

Runx2$^{+/-}$ 두개쇄골이형성증 마우스에서 히스톤 탈아세틸화효소 억제에 의한 뼈 이상 회복 기전 연구

지도 교수 류 현 모

이 논문을 치의과학박사 학위논문으로 제출함

2017년 4월

서울대학교 대학원

치의과학과 분자유전학 전공

배 한 솔

배한솔의 치의과학박사 학위논문을 인준함

2017년 6월

위 원 장 _____ (인)

부위원장 _____ (인)

위 원 _____ (인)

위 원 _____ (인)

위 원 _____ (인)

ABSTRACT

Mechanism of recuing *Runx2* haplodeficiency-induced cleidocranial dysplasia by histone deacetylase inhibition

Han-Sol Bae

Department of Molecular Genetics

The Graduate School

Seoul National University

(Directed by Prof. Hyun-Mo Ryoo, D.D.S., Ph.D.)

Runx2 is a key transcriptional factor of early osteogenesis. Abnormally expressed Runx2 due to disturbance of transcription and post-translational regulation is closely associated to various bone disease. In this study, we focused on cleidocranial dysplasia (CCD) and studied efficacy of drugs in terms of molecular biology and epigenetics to recover the disease.

CCD is a genetic skeletal disorder primarily affecting the development of the bones which is caused by Runx2 haploinsufficiency. As it follows autosomal dominant inheritance pattern, even if one of the parents has a disease, it can be inherited to a child with a 50% probability. Most of CCD patients have symptoms that defective clavicles and large fontanellels due to delayed skeletal development. Generally, it is caused by *Runx2* haploinsufficiency. Numerous studies have

investigated RUNX2 function in bone development and osteoporosis; to date, however, no therapeutic strategy has been proposed for CCD. Therefore, we try to discover a way to overcome the disease with therapeutic regimen. Previous report suggests that there is a critical threshold of *Runx2* mRNA level for the development of CCD phenotypes. Based on these findings, we assumed that the phenotypes of CCD could be relieved when the functional Runx2 which have normal transcription activity is induced up to a certain degree in the patient.

In part I, we showed that *in utero* treatment of MS-275 which is kind of a class I histone deacetylase (HDAC) inhibitor, prevented delayed ossification of calvarial bones in *Runx2*$^{+/-}$ mice a model animal of CCD. Through several experimental analysis, we demonstrated that this effect was mediated via two different mechanisms: 1. post-translational acetylation of Runx2 protein, which proevented the protein from proteosomal degradation and then promoted its transacting activity; 2. increased expression of *Runx2* and osteogenic bone marker genes through epigenetic regulation. In addition, we reveal that MS-275 promotes proliferation of osteoblast both *in vitro* and *in vivo* implying that delayed closure of cranial sutures in CCD is strongly associated with the reduced number of osteoprogenitor cells in frontal area as well as the delayed osteogenesis. In this study, we were able to identify the pathogenic mechanism of CCD and suggested the possibility of treating it with pharmacotherapy.

Next, in part II, we carried out gene expression analysis by RNA-sequencing in primary mouse calvarial cells to validate the *in vivo* results from part I. Through

the Bioinformatics technique, we were able to examine the in vitro changes by *Runx2* deficiency and MS-275 treatment at the genomic level. Thereby, we could make linkage between skeletal development and regulation of gene expression.

Collectively, we demonstrate here that MS-275 exerted its specific therapeutic effect by promoting proliferation, induction ability of osteoblast differentiation and regulating extracellular matrix of osteogenic front cells in the suture region. These results from this study provide the prospective advantages of the therapeutic approach using of MS-275 to alleviate symptoms of CCD and understanding of functional role of MS-275 on osteoprogenitor cells during osteogenesis.

Keyword : Cleidocranial dysplasia, Histone deacetylase inhibitor, MS-275, Runx2, Osteogenesis, Skeletogenesis
Student Number : 2011-22042

Table of Contents

List of Tables

List of Figures

I. LITERATURE REVIEW

I.1. Skeletogenesis

Skeletogenesis is an important process in vertebrates to generate and maintain skeletal structure. The skeleton plays critical roles in supporting muscle, protecting vital organs, affording niche for cells in the immune system, and regulating metabolism as an endocrine and mechanical organ[1-3]. During development and regeneration, bones go through two distinct processes; endochondral ossification and intramembranous ossification[4]. In the process of endochondral ossification, firstly it requires to form a cartilaginous template by mesenchymal stem cells (MSCs) condensation which undergo differentiation into chondrocytes. Sequentially proliferated and matured chondrocytes form cartilage matrix, recruit osteoblast and allow vascularization. Mature osteoblast secretes collagens and other bone-specific proteins to produce new organic matrix which finally mineralized when the physiological signals brought via the circulation. By contrast, intramembranous bone formation arises from directly differentiated osteoblast from condensation of MSCs and neural crest progenitor cells. Subsequently, the matured osteoblasts express extracellular matrix genes including type I collagen, *Osteopontin* (*Opn*; referred to as *Spp1* in Mouse Genome Informatics) and *Osteocalcin* thereby synthesize bone matrix[5].

As the great majority of the organic matrix is collagen, it provides tensile strength. During ossification progresses, hydroxyapatite accumulates in the organic

matrix and calcification occurs, which provides compressive strength. Thus, matured bones are excellent composite material with a combination of collagen and minerals that have physical rigidity and flexibility.

I.2. Runx2 in the process of osteoblast differentiation

Osteoblasts are terminally differentiated cells of mesenchymal stem cells which are specialized to forming bone. They synthesize condensed, cross-linked collagen and a number of functional proteins to constitute the organic matrix of bone. Therefore, for osteoblast maturation, it is necessary osteoprogenitors must express appropriate genes in a timely manner during differentiation progress. Gene expression is finely regulated by transcription factors such as Osterix and Runx2 and the orchestrated activation of various physiological signals. Currently, epigenetic regulation has also been reported as a major regulatory mechanism of gene expression.

Runt-related transcription factor 2 (Runx2/Cbfa1, AML3) is involved in osteoblast-specific member of the Runt transcription factor family. There are consensus sequences specifically recognized by Runx2 as 5'-PyGPyGGT (Py/A)-3' or 5'-(Pu/T) ACCPuCPu-3' [(6)]. Runx2 is considered as a central transcription factor of osteogenesis as it has extensive spectrum of bone- and cartilage-related genes. In concert with physiological signaling pathways and other osteogenic transcription factors RUNX2 controls the functional activity of osteoblasts through

regulate expression of bone marker genes including osteocalcin, alkaline phosphatase, type I and type X collagen in osteoblasts and chondrocytes [7,8]. Abnormal expression of Runx2 protein or *Runx2* gene has been associated with developmentally compromised skeletogenesis and skeletal disease [9]. Inactivated one allele of *RUNX2* is characterized as the cause of human Cleidocranial dysplasia (CCD), by contrast, excessive expression of *RUNX2* is a hall mark of craniosynostosys caused by constitutively active *FGFR1* mutation [10,11].

Many osteogenic signaling pathways, such as BMP2, FGF2, TGF-β, and PTH, control transcription and functional activity of Runx2 during the early phases of osteogenesis [12]. BMP2 signaling, for instance, upregulates the level of Runx2 by stimulating Runx2 acetylation mediated by p300 and preventing Smurf1-mediated degradation. The combination of signaling, TGF-β and BMP2, induces *Runx2* expression and activated Smads (Smad1, -5, and -8) via physical interaction of BMP2 with Runx2 to drive osteoblast differentiation [13]. In previous work [14-16], we demonstrated that the protein activity and stability of Runx2 are regulated by sequential post-translational modifications (PTMs) including phosphorylation, acetylation, prolyl isomerization, and ubiquitination. Among the PTMs of Runx2, acetylation of specific lysine residues in the COOH-terminal regoin is indispensable to stabilize and activate the function of protein [15,16].

I.3. Cleidocranial dysplasia

Cleidocranial dysplasia (CCD; MIM119600) is a bone-related genetic disease that largely affects the development of the skeletal structures and teeth. This disease is caused by defect in the *RUNX2* gene. Reduced or eliminated the activity of RUNX2 interferes with normal bone and cartilage development give rise to symptoms of CCD. The condition is either inherited from parents with an autosomal dominant manner or occurs by *de novo* mutation. As it is autosomal dominant disease, each child inherit the disease with a 50% chance even though only one of their parents is a patient. The individuals with CCD generally have abnormal tooth eruption, delayed development of cranial bones and clavicular hypoplasia. Furthermore, individuals with CCD are shorter than average height [(17)].

Diagnosis of CCD can be made by a skeletal survey (series of X-ray analysis) for general adult or children. During pregnancy, a risk of fetus can be tested for CCD if the genetic cause of the condition has already been identified in a family member. This prenatal diagnosis can be carry out through DNA analysis of fetal cells isolated from amniocentesis or chorionic villus. CCD can also be diagnosis in a pregnancy by an ultrasound of fetus. The abnormal collarbones would be clearly observed after 14 weeks gestation. Nonetheless, there is nothing to do as a parent before, during, or after a pregnancy to cause CCD in a child. Because there is no specific medicine for bone deformities until now and management is based on each patient's symptom.

The child who diagnosis around 5 year-old age, generally surgical

treatment is necessary to avoid any further worsening of the deformity. When bone density is lower than normal, the patient should take calcium and vitamin D and might start preventive treatment for osteoporosis at a young age. In case of the patient who has severe defects of the cranial vault such as symptoms of brain involvement in the place of skull should wear protective helmets during high-risk activities. If the mother has CCD, caesarian delivery should be performed. Some patient suffering from coxa vara should treated by surgery of corrective femoral osteotomies. If there is brachial plexus irritation with pain, excision of the clavicular fragments can be a therapeutic treatment to alleviate it [18-20].

I.4. Histone deacetylase (HDAC) and Histone deacetylase inhibitor (HDI)

DNA is condensed into form of chromatin with highly structured nucleosome. Nucleosome is a basic structural subunit of chromatin which is comprised of an octamer of four core histone proteins, H2A, H2B, H3 and H4. Histone octamer complex is composed of each pairs of core histones which are coiled around 146 base pairs (bp) of DNA strand [21,22]. Each single molecule of nucleosome is linked by 80 bp length of DNA strand called linker DNA. Through several reports, it is clearly identified that histone proteins are integral and dynamic component of the physical responsible for manipulating gene expression. DNA in resting cells is tightly compacted which prevents accessibility of RNA polymerase

II and transcription factors to their specific binding sites. The chromatin in this state is called as heterochromatin. During activation of gene transcription, on the other hand, the condensed chromatin is released, so called euchromatin and the recognition sequences are revealed to enable binding of the transcription factors. Histone protein modification is important in state conversion of chromatin; Heterochromatin to euchromatin. In general, hyper-acetylation of histone is linked with transcriptional activation, whereas histone hypo-acetylation is correlated with transcriptional inactivation [(23)]. Attaching acetyl group to specific lysine residues in the N-terminal region of the core histone is assumed to neutralize the positive charge and to open chromatin structure for transcriptional factor bindings. The dynamic equilibrium of core histone acetylation of controlled by histone deacetylase (HDAC) and histone acetyl transferase (HAT) [(22)].

HDACs serves as an epigenetic regulator that regulate transcription by deacetylation of lysine residue of the histones. HDACs can also removing acetyl groups from non-histone proteins including Runx2, p53, and Stat3, render them more stable and/or increase localization to nuclear zone. In human and mouse, there are 18 kinds of HDACs which are categorized into four groups (class I, II, III, and IV) according to their function, structure, and subcellular localization. Class I, II and IV are enzymes which have zinc-dependent trait while enzymes involved in class III require NAD+ for enzymatic activity. Class I HDACs (HDAC 1-3, and 8) show ubiquitous expression pattern in most tissue, and usually found in cellular nuclei. A number of studies have shown that enzymatic activity of class I HDAC is

necessary for gene transcription, as well as for DNA replication and repair, and cell survival and proliferation. Contrastively, class II HDACs (HDAC 4-7, 9, and 10) is reported to be expressed more tissue-specific, travel between cytoplasm and nucleus in response to physiological signaling stimulation. Some class II HDACs, HDAC6, for example, are demonstrated as affecting cytoskeletal and tubulin structure. However, most of HDACs in class II has considerably lower enzymatic activity compare with those of class I. The major function of class II HDACs are considered to recruit class I HDACs to regulatory region of target genes with their C-terminal deacetylase domain [(24)]. The sirtuins (Sirts 1-7) belong to class IV HDAC which are involving regulation of genome stability, inflammation, energy metabolism, and aging. HDAC11 is the only member in Class IV that expressed across a variety of tissue, little has been investigated about its role.

HDAC inhibitors (HDI) are collectively referred to as chemicals that are known to inhibit the enzymatic activity of HDAC. Commonly, HDIs belong to one of following six basic structural categories. (1) Short-chain fatty acids (Valproate, Sodium butyrate), (2) Cyclic peptides (FR01228, depsipeptide), (3) Benzamides (MS-275). (4) Hydroxamic acid (Suberoylanilide hydroxamic acid; SAHA, Trichostatin A), (5) Epoxyketones (Trapoxin), (6) Hybrid molecules (CHAP31, CHAP50). Several HDIs have approved from Food and Drug Administration (FDA) for clinical usage in United States. Among them, Valproate is the first HDI which approved for clinical use. It has been used as treatments for epilepsy and bipolar disorder. Romidepsin (Depsipeptide, Istodax) and SAHA (Vorinostat,

Zolinza) were approved for therapeutic use for cutaneous T-cell lymphoma. LBH589 (Panobinostat), MS-275 (Entinostat), ITI2357 (givinostat) are in various stages of clinical trials. The reasons that HDIs show therapeutic efficacy in a wide range of disease can be explained by effective correction of aberrant histone modification. Through HDI treatment, silenced genes such as tumor suppressors are expressed, the protein that has been inactivated is activated and the DNA repair mechanism is inhibit which can stimuli apoptosis. HDI-mediated chromatin relaxation may also make oncogenic cells more vulnerable to DNA damage from chemotherapies or radiation [24,25]. The main reason that HDI is commonly used for cancer treatment is its ability to arrest the cell cycle by induction of p21. HDI perturb the formation of dimers from cyclins and cyclin-dependent kinase. Thereby it leads cell cycle arrest and induces cell differentiation [26].

Numerous studies now indicate that HDIs stimulate osteoblast differentiation both background of *in vitro* and *in vivo*. *Westerndorf* et al. reported that HDAC inhibitors increased production of alkaline phosphatase (Alp) and matrix mineralization of *in vitro*-cultured osteoblastic cells and *ex vivo*-cultured calvaria [27,28]. Some HDIs are demonstrated that increased the expression of *Rankl* and *Osteopontin* in osteoblasts and accelerated osteoblast differentiation which is derived from bone marrow mesenchymal stem cells (BMSCs) by promoting Erk signaling. In contrast to their positive regulatory effects on osteoblast differentiation, HDIs decreased osteoclastogenesis by inhibiting the survival and maturation of osteoclasts. TSA inhibited osteoclasts differentiation from

hematopoietic bone marrow cells and induced apoptosis through increasing $p21^{WAF}$ expression. It has also been reported that SAHA disturbs osteoclastogenesis via activation of the NF-κB signaling. However, recent studies demonstrated that epileptic patients who have been prescribed VPA for a long-term tend to show symptoms of osteopenia/osteoporosis with increased fracture risk. The bone loss mechanism by VPA administration is not clear but deduced that it might be associated with certain characteristics of epilepsy including insufficient calcium intake or lack of vitamin D or low physical inactivity.

II. EXPERIMENTAL TECHNIQUES

1. Cell culture

All cell culture media and antibiotics were from Hyclone (GE Healthcare, Little Chalfont, UK). Cells used in this study were cultured at 37°C, in 5% CO_2. Primary calvarial cells from wild type (WT) and *Runx2*$^{+/-}$ mouse were isolated from P0 mice calvarial bone and cultured in alpha MEM with 10% FBS containing 1% penicillin and streptomycin antibiotics. The osteogenic media for osteoblast differentiation, containing 50 μg/ml ascorbic acid and 5 mM β-glycerophosphate in alpha MEM.

2. Cytotoxicity test and cell proliferation assay

To test the cytotoxicity of MS-275, cells were seeded at a confluence of $2x10^3$ cells in 96-well tissue culture plates, and treated with MS-275 for 48 hr. Water-soluble tetrazolium assay was performed for measurement of the number of viable and proliferated cells by using EZ-CyTox solution (Daeil Lab Service, Seoul, Korea). Experiments were conducted according to the manufacturer's instruction. To examine the rate of induced proliferation, culture the cells in two of 96-well tissue culture dish and measure the cell number at day 1 and day 6 each with same process.

3. Alkaline phosphatase (ALP) staining

Cells were cultured for 3 days to 5 days with or without chemical treatment. Sequentially, cells were washed with phosphate buffered saline (PBS) twice, fixed in solution of 2% paraformaldehyde, and then stained for alkaline phosphatase with staining solution according to the manufacturer's instruction (Sigma, St. Louis, MO, USA)

4. Alizarin Red S (ARS) staining

After primary calvarial cells were cultured in osteogenic differentiation medium for 2 weeks, matrix mineralization was confirmed by Alizarin red S staining which stains calcium deposition. At the end of culture period, the cells were fixed with 70% ethanol for 1 hr, washed with PBS and stained with Alizarin red S solution (Sigma, St.Louis, MO, USA). To quantitatively determine the mineral content of each sample, eluted the stain using 0.5 N HCl containing 5% sodium dodecyl sulfate (SDS), and measured the absorbance at 415 nm wavelength.

5. Reverse transcription-polymerase chain reaction (RT-PCR) and Real-time PCR

Cho et al. described detailed experimental protocol previously [29]. Isolated and homogenized calvarial tissues from littermate of WT and *Runx2*$^{+/-}$ mice were prepared follow by RNA extraction. RNA samples were reverse-transcribed by

using the PrimeScript RT kit (Takara Bio, Shiga, Japan). Quantitative real-time PCR was conducted by using Takara SYBR premix Ex Taq (Takara, Shiga, Japan) on an Applied Biosystems 7500 Real Time PCR system (Foster city, CA). Primers were synthesized by Integrated DNA technology (IDT, Coralville, IA). All samples were run in duplicate, and the relative expression levels of mRNA were normalized to those of glyceraldehyde-3-phosphate dehydrogenase (*Gapdh*). The primer sets for real-time PCR in this study are listed in Table 3.

6. Western blot analysis and immunoprecipitation

Cellular proteins from primary calvarial cells were extracted in a lysis buffer which consisting of 150 mM NaCl, 50 mM HEPES (pH 7.5), 100 mM NaF, 1mM EDTA, 0.25% sodium deoxycholate, 1 mM DTT, 0.25% CHAPS, 1% Nonidet P-40, and 10% glycerol supplemented with protease and phosphatase inhibitors, including Na3VO4. For the purpose of measuring the acetylation level, the buffer should be supplemented with 1 mM NaB as previously described [(15)]. Antibodies used for this experiment are listed in Table 1.

7. Immunofluorescence

The process of antigen retrieval is required for immunofluorescent detection of Runx2. The specimens for Runx2 detection were fixed in 4% formaldehyde and boiled for antigen retrieval in Tris/EDTA buffer (pH 9.2) presence of 5% urea for

10 min. The cells were then treated with the primary antibody which detect Runx2 or only IgG as a negative control and stained with fluorescent-conjugated secondary antibody. Visualization was equipped with a Carl Zeiss LSM700 confocal microscope, and analyzed with associated software program, ZEN2011 (Carl Zeiss, Oberkochen, Germany) [30].

8. Immunohistochemistry

For immunohistochemistry, newborn mice were fixed in 4% paraformaldehyde solution for 24 hr and dehydrated, and then embedded in paraffin using standard procedures. Serial paraffin sections (5 μm thicknesses) were prepared, and analyses of immunohistochemical samples were conducted with the Dako Cytomation Envision System (Dako, Glostrup, Denmark). The tissue samples which completed staining procedure were visualized on a conventional microscope operated with a DP72 digital camera (Olympus, Tokyo, Japan).

9. Plasmid construction

The construction of rat *osteocalcin (OC)* –Luc promoter and 6XOSE2-Luc reporter plasmids has been described previously [15,31]. Myc-tagged Runx2 expression vector was kindly provided by Prof. SC Bae in Chungbuk National University.

10. Luciferase assay

The transcriptional activity of Runx2 protein was measured with the constructions of the rat *Osteocalcin* promoter-Luc or 6xOSE2-Luc reporter plasmid vectors. Cells were transfected transiently with the indicated plasmids. Transfection were operated through electroporation technique. 24 hr after transfection, MS-275 or vehicle was treated on cells followed by the measurement of luciferase activity after an overnight incubation. For luciferase assay, cellular lysates were prepared with passive lysis buffer (Promega, WC, USA). After treatment of substrate from Bright-Glo^{TM} Luciferase system (Promega, WC, USA), luciferase activity was detected with a GloMax-Multi Detection System machine (Promega, WC, USA).

11. Chromatin immunoprecipitation (ChIP) assay

ChIP assays in this study were performed with primary mouse calvarial cells that were grown with or without MS-275. Prior to harvest, cells were incubated for 10 min at room temperature in incomplete medium which is containing 1% formaldehyde. Cells were washed and harvested in ice-cold PBS containing protease inhibitors (1 mM phenylmethylsulfonyl fluoride, 1 mM leupeptin, 1 mg/ml pepstatin A, 10 mg/ml TPCK, 4 mg/ml bestatin, 17 mg/ml calpain, 1 mg/ml E64, and 10 mM sodium butyrate). Cell pellets were resuspended in SDS lysis buffer (1% SDS, 50 mM Tris-Cl, pH 8.1, 10 mM EDTA, with protease inhibitors as written above) for 10 min on ice. Samples were sonicated to fragmentation of

the DNA length to 0.1–0.6 kbp (median length 0.4 kbp). After centrifugation of each samples, the supernatant was diluted 10-fold in dilution buffer (0.01% SDS, 1.2 mM EDTA, 1.1% Triton X-100, 16.7 mM NaCl, 16.7 mM Tris-Cl with pH 8.1,) supplemented with a protease inhibitor mixture. Next, DNA-coated protein A/G-agarose was prepared by incubating 500 μl of beads with dilution buffer containing sonicated DNA of 10 mg/ml salmon sperm at 4 °C with agitation for 1 hr. Excess DNA was removed by centrifugation followed by four times consecutive washes of the beads with dilution buffer. Immunoprecipitation was performed with the acetylated histone H4 or methylated histone H3 antibodies in a 1:100 dilution. A non-specific antibody against the unassociated hemagglutinin epitope tag was used as a negative control. After antibody treatment, samples were digested with RNase A (10 mg/ml) at 37 °C for 1 h and proteinase K (20 mg/ml) at 42 °C for 2 h to eliminate RNA and proteins, respectively. Next, the DNA was recovered by DNA extraction kit (Cosmogenetech, Seoul, Korea). An aliquot of each fraction of DNA was used for PCR.

12. Methyl-Specific PCR (MSP)

Genomic DNA from cells for experiment was prepared by cellular DNA extraction using the LaboPass tissue miniprep kit (Cosmo Genetech, Seoul, Korea). The bisulfite conversion was conducted with EpiTect Fast DNA Bisulfite kit (Qiagen). Methyl-specific PCR (MSP) was performed using the Lugen™ Sensi 5xPCR

premix solution (Lugen Sci Co., Seoul, Korea). The primer sets used for this study are listed in Table 3. Primer design for MSP was performed based on the Methprimer software (Li and Dahiya, 2002). Targeting sites of each primer are illustrated in Figure 8. The PCR band intensity which generated by MSP was measured with ImageJ software (National Institutes of Health, Bethesda, MD), and expressed as the percentage of methylation which is able to show the ratio of methylated DNA to unmethylated DNA in target region of gene. The software program named EMBOSS CpG Plot (http://www.ebi.ac.uk/emboss/cpgplot) was used to figure out the region of CpG islands within target gene. All experiments in this study were performed with primary mouse calvarial cells

13. In vitro methylation assay

Runx2 promoter vector was used for this assay. Methylated reporter vectors were prepared through incubating the vector with M.SssI enzyme which works as a CpG methyltransferase (New England BioLabs, Beverly, MA) with treatment of the S-adenosylmethionine (SAM) for 8 hr, at 37 °C, which is following the manufacturer's instructions. The levels of DNA methylation was identified after measure the resistance toward digestive enzyme, HpyCH4IV (New England BioLabs, Beverly, MA) through agarose gel electrophoresis.

14. Animal experiments

Experimental mice with *Runx2*-deficient genotype were generated as described previously [32] and kept under specific pathogen-free (SPF) conditions in animal laboratory of Seoul National University. WT and *Runx2*$^{+/-}$ mice were mated to obtain genotype-matched littermates which expected to have equal ratios of both genotypes. Pregnant mice at 14.5 d.p.c. were injected with 10 mg/kg MS-275 (Calbiochem, Darmstadt, Germany) intraperitoneally. The dose of MS-275 to administrate is decided after toxicity test by checking weight change during pregnancy and number of littermates. Fetal or newborn mice were sacrificed for each experiment. All animal studies were reviewed and approved by the Special Committee on Animal Welfare, Seoul National University, Seoul, Republic of Korea.

15. Skeletal staining

For skeletal staining, E17.5 Embryos or P0 newborn mice were exenterated, skin was peeled follow by fat tissue was removed. After overnight fixation in ethanol with 95% concentration, samples were stained in alcian blue solution (150 mg Alcian blue, 800 ml 98% ethanol, 200 ml acetic acid) for 24 hr. Next, 3 additional hours in 95% ethanol, they were transferred to 2% KOH for 24 hr. Overnight staining in Alizarin red solution (50 mg/l Alizarin red in 2% KOH) was sequentially performed and then skeletons of samples were cleared in solution of

1% KOH with 20% glycerol and gradually increase the amount of glycerol for 2-3 week and stored in 100% glycerol as a final step.

16. Micro CT analysis

After the MS-275 injection, embryonic mice or P0 postnatal mice were sacrificed and performed fixation with 4% paraformaldehyde solution for 24 hr. (depends on size of sample) at 4 °C. Micro-CT scanning was equipped with inspeXio SMX-100CT and analysis was conducted with TRI/3D-BON which is associated software program of inspeXio SMX-100CT (Shimadzu, Kyoto, Japan). After taking 3-dimenational images of micro-CT, samples were sequentially used for immuno-histochemistry or skeletal staining.

17. Calvarial organ culture

E17.5 mice calvaria were dissected and covered skin was removed follow by cultured in a Trowell-typed organ culture-specific dish. Calvarial explants were placed on Nucleopore filters with 0.1-mm pore size and cultured for 48 hr in osteogenic differentiation media presence or absence of 1μM MS-275 in a humidified and sterilized cell incubator with 5% CO2 in air at 37℃. The culture medium was freshly changed every two days. After 48 hr. organ culture progress, harvested explants were fixed in 4% paraformaldehyde (PFA) and performed serial dehydration with a graded concentration of ethanol. After dehydration, explants

were embedded in paraffin wax follow by sectioned to a 5 μm thickness.

18. Double Fluorescence labeling

Double fluorescence labeling assay was operated to determine new bone growth in organ culture system. The Pregnant mice were got intraperitoneal injection with primary labeling reagent, calcein (1 mg/ml, Sigma , St. Louis, MO, USA) in 2% sodium bicarbonate solution 1 day before sacrifice, following by calvarial tissue were isolated from each embryo for organ culture. During organ culture, 0.09 mg/ml of alizarin complexone (Sigma , St. Louis, MO, USA) was supplied to the culture medium for secondary labeling. Double labeling samples with calcein-labeled tissue (green-colored fluorescence) which indicates embryonic mineralization and alizarin complexone-labeled tissue (red-colored fluorescence) which represents mineralization were obtained from this technique. After tissue processing procedures, the labeled fluorescence was visualized on the confocal microscope.

19. Statistical analysis

All quantitative data are presented as means ± SD. Each experiment was performed at least three times, and results from individual representative experiments are shown in figures. Statistical differences were analyzed by Student's *t*-test. $p \leq 0.05$ was considered to indicate a significant difference.

20. RNA-seq. procedure and data analysis

In part I, calvaria of E17.5 mice which treated fetal administration of MS-275 or vehicle at E14.5 and E16.5 were eviscerated in biological triplicate and total RNA was extracted using the Qiazol reagent (Qiagen, Hilden, Germany). In part II, primary calvarial cells were isolated from postnatal day 2 (P2) mice. Isolated primary cells were cultured in presence or absence of 1μM MS-275 for 24hr and treated additional MS-275 or vehicle with osteogenic media at day 3 for 24 hr. Same protocol with part I for RNA isolation was performed. The mRNA in total RNA was converted into a library of template molecules which is appropriate for cluster generation using the Illumina TruSeq RNA Sample Preparation Kit. The TruSeq RNA libraries were quantitated by qPCR. Using these RNA libraries, paired-end sequencing with 76 bp read length was performed on the NextSeq500 platform (Illumina, San Diego, CA, USA) to generate FASTQ-formatted sequence data. Transcriptome levels were determined from the RNA-seq reads via the following RNA-seq pipeline. First, to cut-off sequencing artifacts and poor quality bases, raw data quality control was conducted using Trimmomatic (v0.33) [(33)] with the following options: PE -phred33 ILLUMINACLIP:TruSeq3-PE.fa:2:30:10 MINLEN:50 Trailing:20. Reads were mapped to the mouse genome reference (MM10) from the Ensembl database using Tophat2 (v2.1.0) [(34)]. Conversion and sorting of the alignment file was performed using Samtools (v 0.1.19) [(35)]. The HTseq package [(36)] was used to estimate the count of uniquely mapped reads for each of the 39,179 annotated genes in the gene transfer format (.GTF) file. From

this RNA-seq analysis pipeline, we obtained the expression level of 39,179 genes from 12 samples. The *edgeR* tool was used to detect differentially expressed genes (DEGs), which were classified as either up- or down-regulated depending on fold change. The DAVID Bioinformatics Resource 6.7 (NIAID, NIH) was used for Gene Ontology (GO) pathway analyses.

Table 1. Antibodies used in this study.

Antigen	Clone	Cat.#	Host	Application	Source
Runx2	**8G5**	**D130-3**	**M, mAb**	**WB,IP,IC,IHC, ChIP**	**MBL**
Acetyl-lysine	**-**	**#9441**	**Rb, pAb**	**WB, IP, IHC,IF**	**Cell Signaling**
Histone H3	**-**	**Ab1791**	**Rb, pAb**	**WB, IP, IHC, IF, ChIP**	**MBL**
β-actin	**C-4**	**Sc-47778**	**M, mAb**	**WB, IHC, IP, IHC, IF**	**Santa Cruz**
Acetyl-H4		**17-630**	**Rb, pAb**	**WB, ChIP**	**Millipore**
Methyl-H3K9		**17-680**	**M, mAb**	**WB, ChIP**	**Millipore**
MeCP		**Ab2828**	**Rb, pAb**	**WB, IP, IHC, ChIP**	**Abcam**

M, mouse; Rb, rabbit; G, goat

mAb, monoclonal antibody; pAb, polyclonal antibody

Table 2. Chemical reagents used in this study.

Chemical reagents	Application	Source
DMSO	**Pin1 inhibitor**	**Calbiochem**
MS-275	**HDAC1,3 inhibitor**	**Calbiochem**
CHX	**Protein synthesis inhibitor**	**Sigma-Aldrich**
Calcein	**Green fluorescence labeling reagent**	**Sigma-Aldrich**
Alizarin complexone	**Red fluorescence labeling reagent**	**Sigma-Aldrich**

DMSO, Dimethylsulfoxide; VPA,Valproic acid; SAHA, suberoylanilide hydroxamic acid; CHX, Cycloheximide

Table 3. Primer list used in this study.

For Real-time PCR	
Name	**Oligonucleotide Sequence**
Alp(forward)	*5'- CCA ACT CTT TTG TGC CAG AGA-3'*
Alp(reverse)	*5'- GGC TAC ATT GGT GTT GAG CTT TT -3'*
Osteocalcin (forward)	*5'- CTG ACA AAG CCT TCA TGT CCA A -3'*
Osteocalcin (reverse)	*5'- GCG CCG GAG TCT GTT CAC TA -3'*
Collagen1α1(forward)	*5'- GCTCCTCTTAGGGGCCACT - 3'*
Collagen1α1 (reverse)	*5'- CCACGTCTCACCATTGGGG -3'*
Runx2 (forward)	*5'-TTC TCC AAC CCA CGA ATG CAC -3'*
Runx2(reverse)	*5'-CAG GTA CGT GTG GTA GTG AGT -3'*
Bmp2(forward)	*5'-GGGACCCGCTGTCTTCTAGT-3'*
Bmp2(reverse)	*5'-TCAACTCAAATTCGCTGAGGAC -3'*
β-catenin(forward)	*5'-ATGGAGCCGGACAGAAAAGC -3'*
β-catenin (reverse)	*5'-CTTGCCACTCAGGGAAGGA -3'*
Pcna(forward)	*5'-TTTGAGGCACGCCTGATCC -3'*
Pcna(reverse)	*5'-GGAGACGTGAGACGAGTCCAT -3'*
Cyclin D1(forward)	*5'-CCA AAA TGC CAG AGG CGG ATG AG -3'*
Cyclin D1(reverse)	*5'-CTA CCA TGG AGG GTG GGT TGG AA -3'*
Mapk(forward)	*5'-CAGGTGTTCGACGTAGGGC -3'*
Mapk(reverse)	*5'-TCTGGTGCTCAAAAGGACTGA -3'*
For ChIP assay	
Runx2 (forward)	*5'-CGAGGCTGCGAGCTAGAC-3'*
Runx2 (Reverse)	*5'-CTCCTCCGCCTCCTCCTC-3'*
For Methyl-specific PCR	
Runx2, Methylated (Forward)	*5'-AAGTTTGTAAAAATTTGTTTTTCGT-3'*
Runx2, Methylated (Reverse)	*5'-CTCAAACTACTCCGACTAACGTT-3'*
Runx2 Unmethylated (Forward)	*5'-AAGTTTGTAAAAATTTGTTTTTTGT-3'*
Runx2 Unmethylated (Reverse)	*5'-ACCTCAAACTACTCCAACTAACATT-3'*

Table 4. The number of mice used in each experiment.

		Skeletal staining (E16.5)	Skeletal staining (P0)	µCT (Single injection) & Histology	µCT (Multiple injection) & Histology	Double fluorescence stainig	RNA works	
Geno type	**Treat ment**	**The number of mice**						**Total**
WT	**Veh.**	**31**	**12**	**23**	**23**	**17**	**9**	**115**
	MS.	**35**	**7**	**9**	**19**	**10**	**16**	**96**
***Runx2*$^{+/-}$**	**Veh.**	**51**	**8**	**23**	**14**	**21**	**14**	**131**
	MS.	**24**	**3**	**11**	**17**	**15**	**7**	**77**
		Total number of mice						**419**

Veh.; Vehicle. MS.; MS-275

III. PART I

Journal of Bone and Mineral Research, 4 January 2017, accepted

An HDAC inhibitor, Entinostat/MS-275, prevents delayed cranial suture closure in heterozygous *Runx2* null mice

Abstract

Cleidocranial dysplasia (CCD) is an autosomal dominant skeletal disorder caused by mutations in *RUNX2*, coding a key transcription factor of early osteogenesis. CCD patients suffer from the developmental defects in cranial bones. Despite numerous investigations and clinical approaches, no therapeutic strategy has been suggested to prevent CCD. Here, we show that fetal administration of Entinostat/MS-275, a class I histone deacetylase (HDAC)-specific inhibitor, partially prevents delayed closure of cranial sutures in *Runx2*$^{+/-}$ mice strain of C57BL/6J by two mechanisms: (1) post-translational acetylation of Runx2 protein, which stabilized the protein and activated its transcriptional activity; and (2) epigenetic regulation of *Runx2* and other bone marker genes. Moreover, we show that MS-275 stimulates osteoblast proliferation effectively both *in vivo* and *in vitro* suggesting that delayed skeletal development in CCD is closely related to the decreased number of progenitor cells as well as the delayed osteogenic differentiation. These findings provide the potential benefits of the therapeutic strategy using MS-275 to prevent CCD.

Introduction

RUNX2, the central transcriptional factor of osteogenesis, regulates osteogenic cell proliferation and differentiation [32,37]. In concert with other osteogenic transcription factors, including Osx, Dlx5, and NFI-C, RUNX2 controls the functions of osteoblasts to regulate expression of bone marker genes such as osteocalcin [7,8]. Mouse fetuses harboring targeted disruption of *Runx2* exhibit a complete lack of ossification due to maturation arrest of osteoblasts, indicating that this gene plays an indispensable role at the early stages of osteoblast differentiation [32,38]. The biological and clinical significance of *RUNX2* was established by the identification of a mutation in the *RUNX2* gene locus in humans with cleidocranial dysplasia (CCD), an autosomal dominant skeletal disease [10,11]. The symptoms of CCD include clavicular hypoplasia, delayed development, and ossification of cranial bones. *Runx2*$^{+/-}$ mice exhibit symptoms similar to those of human CCD patients [10,11], indicating the importance of RUNX2 in intramembranous bone formation.

Previously, Lou et al. [39] established a mouse model in which *Runx2* expression can be finely regulated by neo cassette. They found that the *Runx2* mRNA level must drop below a critical threshold for CCD-like phenotypes to develop; mice expressing lower levels of *Runx2* mRNA [55–70% of that in the wild type (WT)] developed CCD-like phenotypes, whereas mice with higher *Runx2* mRNA levels (>79% of WT) developed a normal skeleton. These findings prompted us to hypothesize that symptoms of CCD could be alleviated when

functional *Runx2* transcriptional activity is restored to the threshold level.

Many osteogenic signals, such as BMP2, TGF-β, FGF2, and PTH, regulate Runx2 expression during the early stages of osteogenesis [12]. However, because of their non-specific effects on overall biological processes, it would be challenging to use these growth factors for human treatment. In previous works [14-16], we showed that the stability and transactivation activity of Runx2 protein are regulated by serial post-translational modifications such as phosphorylation, prolyl isomerization, acetylation, and ubiquitination. Accordingly, modulation of one or more of these post-translational modifications of Runx2 represents a therapeutic target for treatment of the genetic disease CCD.

Among the post-translational modifications of Runx2, acetylation of several lysine residues in Runx2 C-terminus is necessary to stabilize and activate the protein [15,16]. Numerous *in vitro* studies illustrated that HDAC inhibitors (HDIs) induces acetylation of both histone and non-histone proteins, including Runx2 [14]. In addition, our previous studies showed that MS-275, an HDI, exerts a strong bone anabolic effect in models of calvarial defect or osteoporosis in adult animals [27,40]. MS-275 is also known by the clinically as Entinostat (Syndax pharmaceuticals Inc. USA) and currently being used in clinical trials for treating cancers. Based on these previous results, we hypothesize MS-275 also exerts a Runx2-mediated anabolic effect in the early stage of bone development in fetal animals. In this paper, we tested our hypothesis by administering MS-275 to *Runx2*-haplodeficient mice, a model for human CCD, and observed the effects of the drug on their developmental

bone defects.

Result

MS-275 restored CCD phenotypes in *Runx2*$^{+/-}$ mice

To determine whether MS-275 can functionally compensate for CCD-like phenotypes in *Runx2*-deficient phenotypes, we established a single-injection regimen in which MS-275 was administered to pregnant mice. According to previous studies, dynamic skeletogenesis in cranial bones occurs between E14.5 and birth [32,38]. Therefore, we administered MS-275 at 14.5 d.p.c. and sacrificed fetuses at 16.5 d.p.c. All fetuses were evaluated for their level of bone developmental using measurements of ossified vertebrae length, ratio of ossified area over whole skull area, and sizes of the mandible and clavicle (Fig. 1A-H). MS-275 treatment had an effect on overall skeletal growth. Ossified vertebral length was 40% shorter in *Runx2*$^{+/-}$ than in their WT littermates, but MS-275 treatment of *Runx2*$^{+/-}$ mice significantly increased their ossified vertebral lengths nearly to WT levels (Fig. 1A, B, $p<0.05$). Similar growth was observed in membranous bones including calvaria, mandibles, and clavicles. MS-275 treatment of *Runx2*$^{+/-}$ mice significantly ($p<0.05$) increased mineralization of these bones nearly to WT levels (Fig. 1C-H). In calvarial bone and mandible, the therapeutic effect of MS-275 was remarkable: *Runx2*$^{+/-}$ traits were recovered almost to the WT level. By contrast, the drug had a relatively small effect on clavicle development,

although the increase in mineralization was still significant ($p<0.05$) and the associated morphological change was meaningful. MS-275–treated clavicles exhibited a more developed skeletal curve, and development of their medial part (i.e., the region attached to sternal bone) was much more prominent than that of the lateral part (i.e., the region arranged with acromial bone) (Fig. 2). Importantly, the medial part of the clavicle arises via intramembranous bone formation, whereas the lateral part is formed by endochondral ossification [41]. These results corresponded well with a previous report showing that Runx2 is more important for intramembranous than endochondral bone formation [32]. Therefore, the rescue of CCD phenotypes by MS-275 treatment is more prominent in intramembranous bone development, as observed in this study.

To determine whether MS-275 treatment affects bone development until they are born, we examined calvarial phenotypes of pups at P0 after single administration of MS-275 to pregnant mice at 14.5 d.p.c. Results of skeletal staining and microCT analysis revealed no significant difference between the MS-275 and vehicle-treated groups (Fig. 3). However, because the half-life of MS-275 is only 1 hr in rodents [42], a single injection may not be pharmacokinetically sufficient to cause medical effects that persist until birth. Therefore, we treated MS-275 twice (14.5 and 16.5 d.p.c.) to minimize toxicity and maternal stress, and confirmed that double injection was effective. Under these treatment conditions, the CCD phenotypes of P0 *Runx2*$^{+/-}$ mice were almost comparably abolished, and the mice were nearly WT in appearance (Fig. 4A-C). In Fig. 4A, we observed that

MS-275 leads bone formation also in WT group. It is compatible with our previous research, which showed therapeutic value of MS-275 in osteoporosis-induced adult mice [40]. Based on these data, it is clear that maintenance of an adequate therapeutic level of MS-275 is critical, and that a well-controlled pharmacokinetic study of its effects should be performed.

To rule out maternal effects of MS-275, we employed a mouse calvarial organ culture system. In Fig. 4D, calcein labeling of calcified tissue *in utero* was observed as green fluorescence, and newly mineralized tissue formed during organ culture was observed as red fluorescence. From these observations, we could estimate growth through the effect of MS-275 treatment alone. MS-275 treatment caused a strong increase in newly generated calvarial bone in both genotypes of mice, but the recovery effect was more dramatic in *Runx2*$^{+/-}$ than in *WT* mice (Fig. 4D). Thus, the distance between osteogenic fronts of parietal bones was closer in the presence of MS-275. The results of coronal sectional view strongly supports this observation (Fig. 1D, E). It is notable that MS-275 stimulates mineralization on the osteogenic front. Therefore, these results indicated that MS-275 is a positive regulator of intramembranous bone formation *in vivo*.

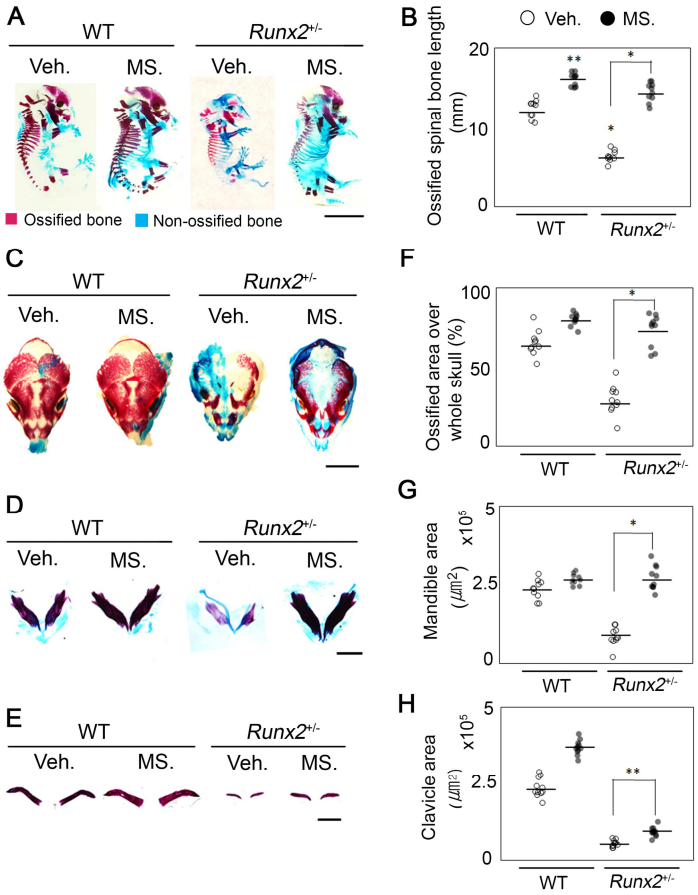

Fig. 1. MS-275 rescues the CCD-like phenotypes in *Runx2*$^{+/-}$ mice. Fetuses were treated with MS-275 or vehicle either once at 14.5 d.p.c. or twice at 14.5 and 16.5 d.p.c. *in utero*. (**A**) Representative skeletal staining of E16.5 WT and *Runx2*$^{+/-}$ mice that received one injection *in utero*. (Scale bar, 5 mm) (**B**) Lengths of ossified spinal bone. The same samples were cut into (**C**) calvaria (Scale bar, 2 mm) and (**D**) mandible (Scale bar, 2 mm) (**E**) clavicles (Scale bar, 1 mm) (**F–H**) Quantitative analysis of each sample is depicted as scatter plot graphs to the right of each figure. Developing clavicles exhibit a significant increase in mineralized area. Quantitative data were obtained using the ImageJ software. Veh.= Vehicle, MS.= MS-275. *P<0.05, **P<0.01, ***P<0.001, Student's *t*-test.

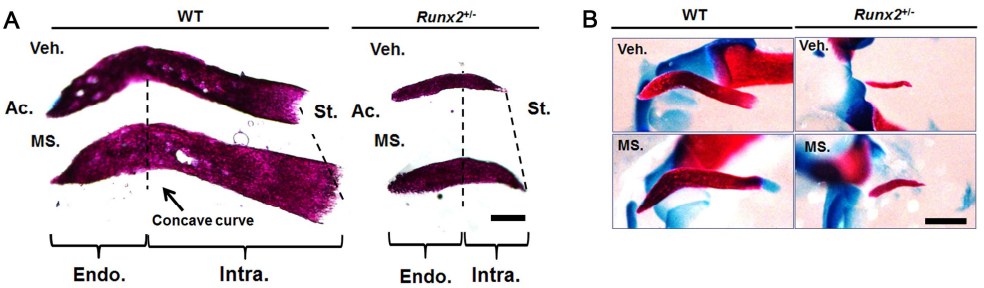

Fig. 2. MS-275 induced intramembranous development of clavicles in both WT and *Runx2*$^{+/-}$ fetal mice. (**A**) Magnified images of Fig. 1E. Dotted lines indicate development of intramembranously formed bone from concave curves. MS-275–treated clavicles exhibited a more developed skeletal curve, and development of their medial part (i.e., the region attached to sternal bone) was much more prominent than that of the lateral part (i.e., the region arranged with acromial bone). Importantly, the medial part of the clavicle arises via intramembranous bone formation, whereas the lateral part is formed by endochondral ossification. These results indicated that the rescue of CCD phenotypes by MS-275 treatment is more prominent in intramembranous bone development. (Scale bar, 200 µm) (**B**) Skeletal staining images were acquired with all bones in their original positions to determine the morphological directions of the clavicles. (Scale bar, 1 mm). Ac: acromial end; St: sternal end; Endo: endochondral ossification; Intra; intramembranous ossification.

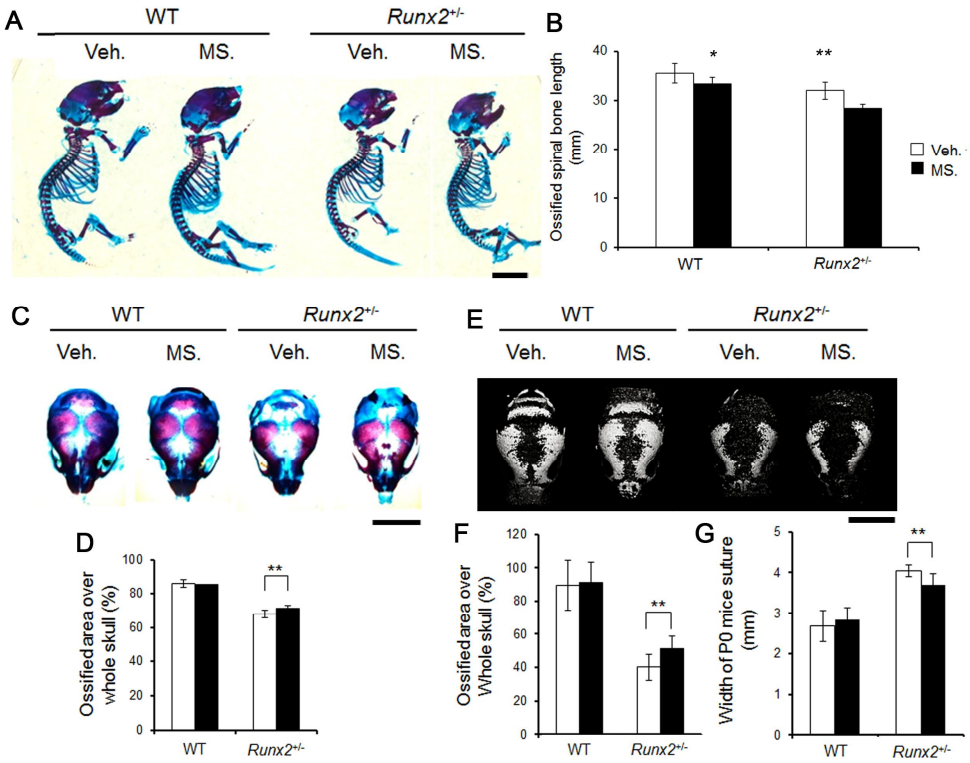

Fig. 3. A single administration of MS-275 had no significant effect on P0 skeletons. (**A**) Representative skeletal staining images of newborn mice. Mice were treated with vehicle or 10 mg/kg MS-275 once at E14.5. Long bone development was not significantly perturbed by *Runx2* deficiency at the postnatal stage. (Scale bar, 5 mm) (**B**) Ossified spinal bone lengths. (**C**) Dissected calvaria from (**A**) (Scale bar, 5 mm). (**D**) Ossification level of each sample. (**E**) Representative microCTs of skulls from newborn WT and *Runx2*$^{+/-}$ mice that received the indicated chemicals at E14.5 (scale bar, 5 mm). Ossification level of each group was measured as (**F**) % of ossified area over full skull and (**G**) distance between parietal bones. Quantitative data were obtained using ImageJ. Data represent means ± SD (n=15 to 20). Data followed a normal distribution. Veh.: vehicle; MS.: MS-275; *P<0.05, **P<0.01, ***P<0.001, Student's *t*-test.

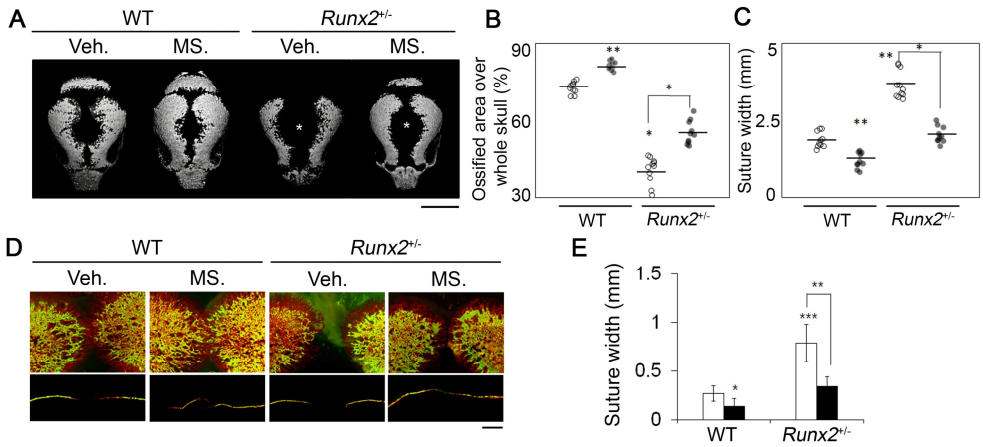

Fig. 4. Multiple administrations of MS-275 show significant effect on *Runx2*$^{+/-}$ mice. (**A**) Representative microCTs of skulls from newborn WT and *Runx2*$^{+/-}$ mice that received the indicated chemicals at E14.5 and E16.5. The asterisk (*) indicates rescue of CCD-like phenotype on calvaria. Ossification level of each group was measured as (**B**) % of ossified area over full skull area and (**C**) width between parietal bones. (**D**) Double fluorescence reveals new bone growth in organ-cultured E17.5 calvarial tissue. The tissue was visualized by fluorescence microscopy as whole tissue (upper) or coronal sections (lower). (Scale bar, 1 mm) (**E**) Suture width of (**D**) was measured. Quantitative data were obtained using the ImageJ software. Veh.= Vehicle, MS.= MS-275. *P<0.05, **P<0.01, ***P<0.001, Student's *t*-test.

MS-275 restores Runx2 protein acetylation and stabilizes its transactivating activity in *Runx2*$^{+/-}$ calvaria cells.

We showed previously that HDIs stabilizes Runx2 by post-translational modification [15]; however, it remains unclear whether it could compensate for Runx2 activity in *Runx2*-deficient organisms. To address this possibility, we examined the changes of acetylated Runx2 level in WT and *Runx2*$^{+/-}$ calvarial cells following MS-275 treatment. Immunoprecipitation and immunoblot analysis showed that acetylation of Runx2 was lower in *Runx2*$^{+/-}$ mouse calvarial cells than in WT cells. By contrast, acetylated Runx2 level of MS-275 treated *Runx2*$^{+/-}$ mouse calvaria cells was restored to that of the WT-vehicle treated group (Fig. 5A). To determine whether MS-275 increases the amount of Runx2 protein, we examined the endogenous Runx2 level. Indeed, the amount of Runx2 increased in a dose-dependent manner upon MS-275 treatment (Fig. 5B, C).

Next, we investigated whether MS-275 stabilizes the Runx2 protein. The degradation rate was lower in the MS-275–treated group than in the vehicle-treated group: specifically, the half-life of Runx2 was 13.02 hr in the absence of MS-275 and 18.15 hr in the presence of MS-275 (Fig. 5D, E). Moreover, immunofluorescence assays revealed that the total Runx2 protein level was elevated in both genotypes of MS-275–treated mouse calvarial cells. In the *Runx2*$^{+/-}$ cells, the expression level of Runx2 protein in nucleus was restored to WT levels (Fig. 5F, G). We observed similar Runx2 expression patterns in mouse calvarial tissue. The amount of Runx2 protein accumulated in the nucleus of

osteoblasts around calvarial bone was elevated in MS-275 treated *Runx2*$^{+/-}$ mouse calvaria (Fig. 6). Because both acetylation and ubiquitination occur at similar lysine residues [43], this observation could be attributed to a protective mechanism that inhibits the ubiquitination and proteosomal degradation pathway.

To determine whether MS-275 affects Runx2 transactivating activity, we carried out reporter assays. The results show that MS-275 up-regulated Runx2 transcription activity in mouse calvarial cells of both genotypes. Remarkably, a high dose of MS-275 restored Runx2 transactivating activity in *Runx2*$^{+/-}$ cells to WT levels (Fig. 7A). Additionally, because *Osteocalcin* is a direct target of Runx2 [44], we investigated the role of MS-275 on Runx2-mediated promoter activity. Runx2 overexpression significantly activated *Osteocalcin* promoter activity, but not the activity of a mutant reporter gene with an altered Runx2-binding site. Runx2 overexpression and MS-275 treatment synergistically stimulated osteocalcin promoter activity. On the other hand, Runx2 overexpression could not stimulate the mutant OC-promoter with the altered Runx2 binding-site mutant, whereas MS-275 could still stimulate the mutant construct (Fig.7B). Based on these observations, we hypothesize that MS-275 might influence on not only Runx2, but also other transcription factors that bind in that region. These results suggest that MS-275 enhances transcription activity of Runx2 via post-translational acetylation of Runx2.

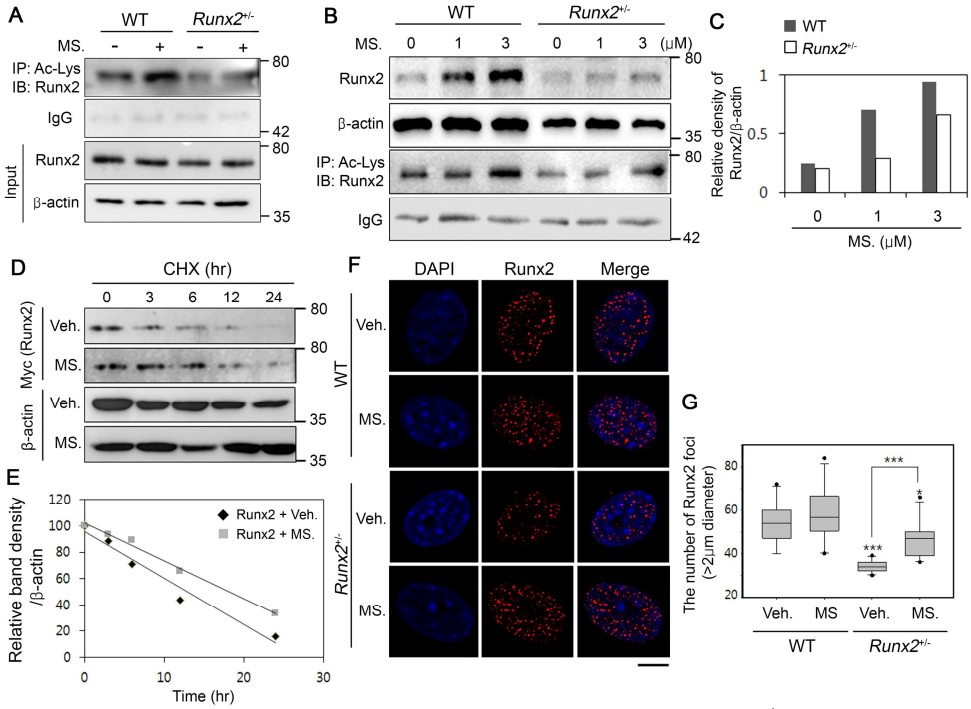

Fig. 5. MS-275 stabilizes Runx2 protein. (**A**) WT and *Runx2*$^{+/-}$ mouse calvaria cells were cultured in the presence or absence of 1 μM MS-275 for 24 hr. Acetylated Runx2 was measured by immunoprecipitation (IP). Since amount of Runx2 in *Runx2*$^{+/-}$ is almost half of that in WT, equal amounts of Runx2 Inputs were estimated and normalized before IP. (**B**) Primary osteoblasts were cultured with MS-275 for 24 hr, and the abundance of endogenous Runx2 protein was examined by IB. (**C**) Protein band intensities in (**B**). (**D**) Following transfection with Myc-tagged Runx2 primary calvaria cells were treated with or without 1 μM MS-275 for 24hr and cultured with cycloheximide (CHX, 10 μg/ml) for the indicated times. Levels of Runx2 were assessed by detecting Myc protein. (**E**) Estimated change of Runx2 expression level over time. (**F**) Runx2 in each genotype of calvarial cells was detected after treatment with 1 μM MS-275 for 24 hr. (Scale bar, 10 μm). (**G**) Number of nuclear Runx2 foci in (**F**). Quantitative data were obtained using ImageJ. Veh.= Vehicle, MS.= MS-275, E.V.= Empty vector, *P<0.05, **P<0.01, ***P<0.001, Student's *t*-test.

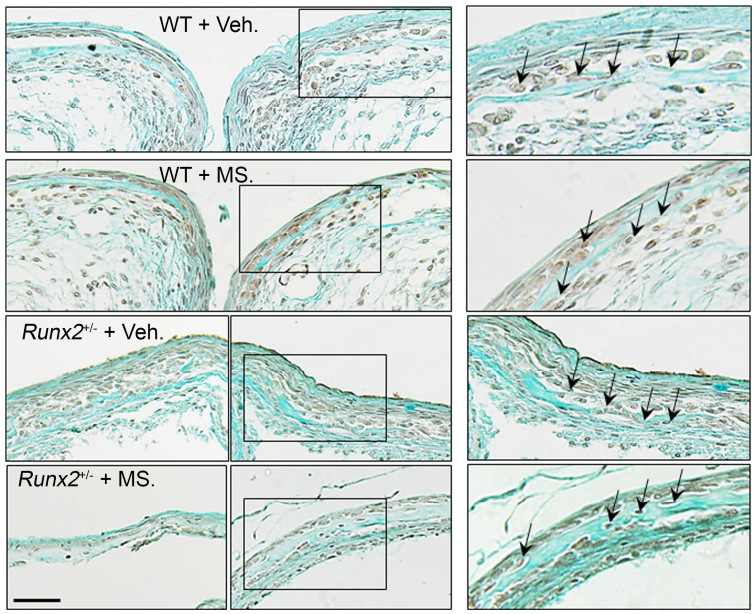

Fig. 6. MS-275 increases amount of Runx2 protein in mouse calvarial tissue. Runx2 levels in P0 mice calvarial tissue were determined by immunohistochemistry. Arrows indicate Runx2-positive osteoblasts. Enlargement of the boxed regions are displayed on the right side.

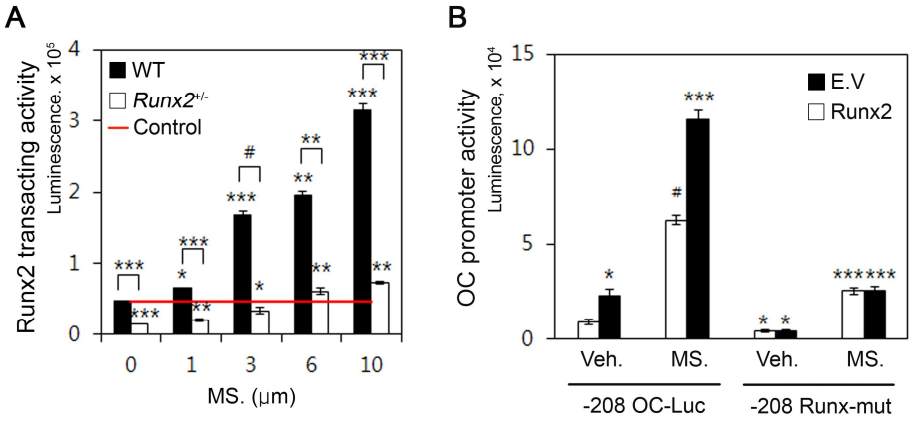

Fig. 7. MS-275 activates Runx2 transacting activity. (**A**) Runx2-transactivating activity following 24 hr treatment of calvarial cells with the indicated dose of MS-275, assessed by luciferase assay using the 6XOSE2 reporter gene. The red line indicates the activity of vehicle-treated WT. (**B**) HEK293T cells were transfected with WT (-208 OC-Luc) or Runx2-binding site mutant osteocalcin (OC) promoter–Luc (-208 RUNX-mut) with or without Runx2 overexpression. Luciferase activity was measured following treatment with 3 μM MS-275 or vehicle for 24 hr. Veh.= Vehicle, MS.= MS-275, E.V.= Empty vector. *P<0.05, **P<0.01, ***P<0.001, #P<0.0001, Student's *t*-test.

MS-275 induces epigenetic regulation of the *Runx2* promoter region

Previous studies showed that MS-275 works as a chromatin modulator (epidrug) on stem cells and affects their potency and differentiation [45]. These observations led us to hypothesize that treatment of MS-275 would change the epigenetic landscape of primary calvarial cells. *Runx2* has at least two different isoforms using alternative promoters, which show differential expression patterns in mouse calvaria development [46]. P1 promoter (Distal) drives transcription of *type-II Runx2 (Runx2-II)* known for bone-specific-expression whereas P2 promoter (Proximal) induces *Type-I Runx2 (Runx2-I)* expression in undifferentiated mesenchymal stem cell, preosteoblasts and chondrocyte precursors. *In silico* analysis predicted the existence of CpG islands in the *Runx2*-P2 promoter region that are conserved among species [47]. These CpG islands are located near the transcription start site. Using that region as an epigenetic target, we measured *Runx2* expression and observed changes in several epigenetic markers[47] (Fig. 8).

First, we confirmed that *Runx2* expression levels in primary mouse calvarial cells were increased by MS-275 treatment (Fig. 9A). To investigate whether MS-275 has an epigenetic function, we performed chromatin immunoprecipitation (ChIP) assays (Fig. 9B). We checked the levels of acetylated histone H4 (Ac-H4), di-methylated histone H3K9 (Me-H3K9) and methyl CpG binding protein 2 (MeCP2) [48]. The level of acetylated histone H4 (Ac-H4), a hallmark of transcriptionally activated genes [49], was increased by MS-275 treatment. By contrast, the levels of methylated H3K9 (Me-H3K9) and methyl

CpG binding protein 2 (MeCP2) binding, both of which are markers of epigenetic suppression [50], decreased following MS-275 treatment (Fig. 9B). Methylated histones control skeletal development, and down-regulation of histone methylation in osteoblasts increases bone formation [51,52]. The results of the ChIP assay revealed genomic interactions of epigenetic factors with the *Runx2* promoter region; these interactions finely reflect the trend of *Runx2* expression as shown in Fig. 9A. Thus, we were able to deduce MS-275 activates *Runx2* promoter.

Next, we carried out methylation-specific PCR to measure the DNA methylation status of the *Runx2* promoter. Usually, hypermethylated DNA indicates a transcriptionally inactivated state [53]. We found that MS-275 treatment decreased the amount of methylated PCR products and increased the amount of unmethylated-DNA fragments in primary calvarial cells. Thus, MS-275 causes hypomethylation of 5'-cytosine in CpG islands of the *Runx2-I* promoter (Fig. 9C). *Runx2* gene expression (Fig. 9A) was inversely correlated with the methylation level of the CpG island in *Runx2* promoter (Fig. 9C). This result also suggested that *Runx2* was transcriptionally activated by MS-275. To confirm the ability of MS-275 to activate the *Runx2* gene, we performed an artificial *in vitro* methylation assay using M.SssI methyltransferase, as previously described [54]. The *HpyCH4IV* restriction enzyme was used to validate promoter construct methylation: this enzyme recognizes the sequence ACGT and cuts selectively at sites containing unmethylated cytosine, but cannot cut at CpG sites methylated by M.SssI (Fig. 9D). To assess the functional effects of MS-275 on CpG-methylated gene expression,

we analyzed *Runx2* promoter activity in luciferase reporter assays using *in vitro* methylated or unmethylated constructs. We found that a construct inactivated by CpG methylation was activated by MS-275 in a dose-dependent manner (Fig. 9E). These results also correspond with patterns of *Runx2* expression (Fig. 9A) and CpG methylation (Fig. 9C). In aspects of histone modification, our results of ChIP assay and immune blot assay were also comparable with previous study, which demonstrated marked histone modification dynamics during osteoblast differentiation (Fig. 9B, Fig. 10). In the process of osteogenesis, promoter region of *Runx2* experienced elevated H3 and H4 acetylation and reduced H3K9, H3K27 methylation whereas global level of those hall marks were not changed [48]. Altogether, our *in vitro* results suggest that MS-275 induced *Runx2* expression by affecting the epigenetic landscape of the *Runx2* promoter region, which might increase the potential of primary calvarial cells to develop into mature osteoblasts.

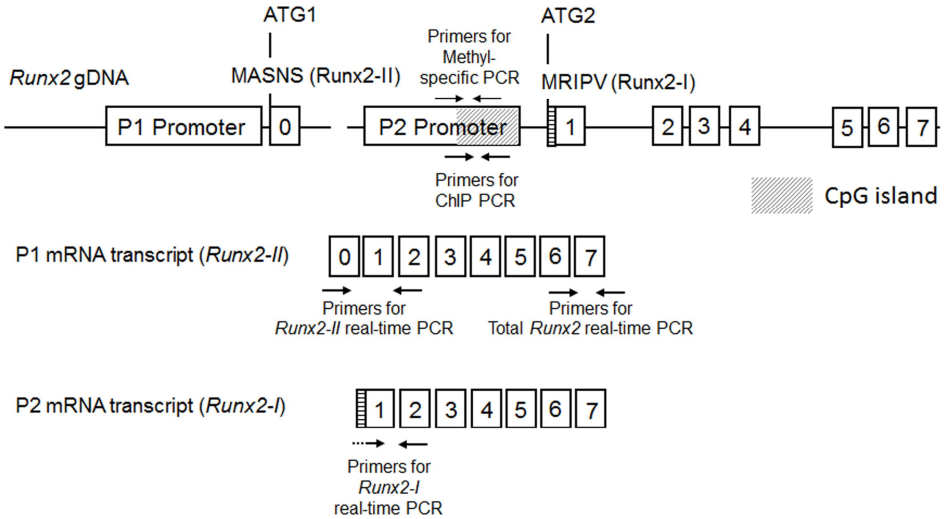

Fig. 8. The structure of *Runx2* genome and derived transcripts. The *Runx2* gene consist of eight exons and two alternative promoters; P1 and P2 promoter. P1 is a distal promoter which regulates the transcription of *type-II Runx2* coding type-II Runx2 protein starting at MRIPV amino terminus. P2 is a proximal promoter involved in *type-I Runx2* expression coding type-I Runx2 protein containing MASNS amino terminus. CpG island is located at the region of P2 promoter. The diagram is showing the overall targeting sites of primers study for RT-PCR, Methyl-Specific PCR, and ChIP-qPCR. Sequence of each primers are indicated in Table. 3.

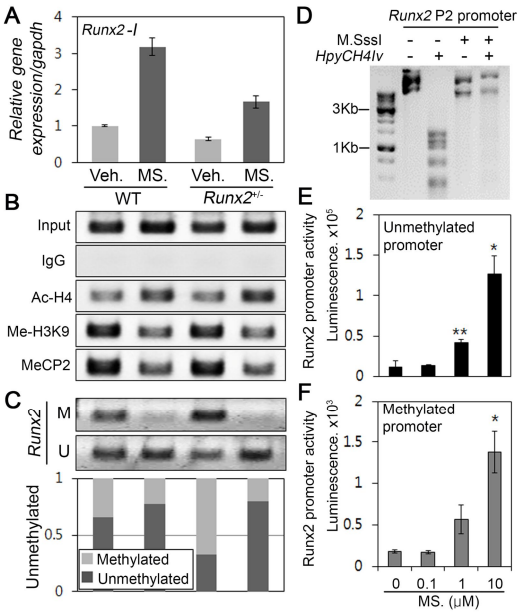

Fig. 9. MS-275 enables epigenetic modification of the *Runx2* P2 promoter, resulting in elevated expression. (**A–C**) WT and *Runx2*$^{+/-}$ primary osteoblasts were treated with vehicle or 3 μM MS-275 for 24 hr. (**A**) *Runx2-I* levels were determined by qPCR. (**B**) ChIP assays were carried out using antibodies against H4 Ac, H3K9 Me, and MeCP. Chromatin fragments were PCR-amplified with primers for *Runx2*. (**C**) MSP analysis of the *Runx2* promoter region. M and U represent amplification of methylated and unmethylated alleles, respectively. Bottom panel: Quantitation of MSP band density for unmethylated genes (dark gray bar) and methylated genes (light gray bar). (**D**) Digested or non-digested bands of *Runx2* P2 promoter luciferase reporter vector after *HpyCH4IV* endonuclease treatment, to confirm *in vitro* hypermethylation status. Methylation on the cytosine residue was carried by M.SssI CpG methyltransferase. (**E–F**) *Runx2* promoter activity was assessed by luciferase reporter activity of (**E**) unmethylated promoter construct and (**F**) hypermethylated promoter. WT mouse calvarial cells were transfected with a *Runx2* P2 promoter reporter construct, followed by the indicated dose of MS-275 treatment for 24 hr. *P<0.05, **P<0.01, Student's *t*-test.

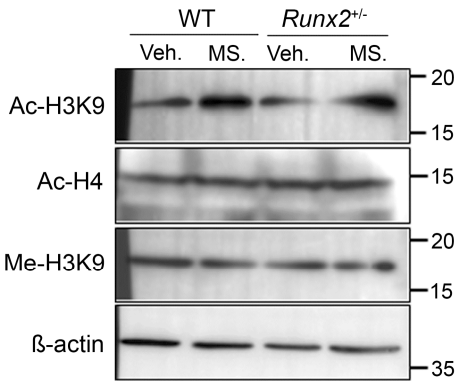

Fig. 10. Global levels of histone modifications. Histone samples were collected after 3μM MS-275 treatment to WT and *Runx2*$^{+/-}$ primary calvarial cells. Primary mouse calvarial cells were cultured with or without 3 μM MS-275 for 24 hrs and general levels of histone modifications were detected by immunoblot. Histone 3 and beta-actin were used as loading controls. The bands of ß-actin were detected as a loading control.

MS-275 accelerates osteoblast differentiation by activating proliferation and inhibiting apoptosis

As we showed in Fig. 5, MS-275 induced Runx2 acetylation, thereby generating the activated form of Runx2, which positively regulates cell proliferation and differentiation. Previously, we showed that proliferation of osteoblast precursor cells in osteogenic front regions is a critical mechanism underlying suture closure [55]. Furthermore, several reports suggest that suppression of HDAC1 increases cell proliferation and global protein synthesis in osseous cells [45,56]. Because MS-275 is a member of selective class I HDAC inhibitors, we expected that treatment of MS-275 would improve proliferative activity of calvarial cells and affect osteoblast differentiation. Therefore, we performed RNA-seq to investigate the action of MS-275 on fetal calvaria and assess their transcriptomic response. GO term analyses revealed that administration of MS-275 affected various biological processes (Fig. 11A). Enrichment for GO terms associated with chromatin modification (GO:0016568), skeletal development (GO:0001501), and regulation of proliferation (GO:0042127) support previously characterized roles of MS-275. The Venn diagrams shown in Fig. 11B show 4127 up-regulated genes and 6057 down-regulated genes (95% confidence, Student's *t*-test), of which 430 up-regulated and 218 down-regulated genes overlapped between E17.5 WT and *Runx2*$^{+/-}$ calvaria (Fig. 11B). Table 5 shows representative hallmark genes, grouped according to biological process. In general, genes related to bone formation and proliferation were up-regulated, whereas genes related to apoptosis were down-

regulated. Firstly, we examined the *in vitro* effects of MS-275 on process of osteoblast differentiation. Expression levels of bone marker genes were elevated, indicating that MS-275 treatment rescued gene expression in *Runx2*$^{+/-}$ cells (Fig. 12A). We investigated the early stages of osteoblast differentiation using ALP staining. MS-275 potentiated ALP activity in a dose-dependent manner in both WT and *Runx2*$^{+/-}$ cells. ALP staining levels were lower in *Runx2*$^{+/-}$ cells than in WT cells, but were increased by a high dose of MS-275: specifically, the staining level in *Runx2*$^{+/-}$ cells exposed to 6 μM MS-275 were similar to those of vehicle-treated WT cells (Fig. 12B). In accordance with the elevated ALP activity, MS-275 also increased calcium deposition, as determined by Alizarin Red S staining, which can show the late stages of osteoblast differentiation (Fig. 12C). These results are consistent with our assumption that MS-275 would compensate for the delayed differentiation potency of *Runx2*$^{+/-}$ cells.

Next, we examined the effects of MS-275 on cell proliferation. Expression levels of proliferation marker genes were slightly elevated, as shown in Table. 1. Notably, expression of *β-catenin (Ctnnb)* and *Cyclin D1 (Ccnd1)* (Fig. 13A) is linked with suture closure [(57)]. Immunohistochemistry revealed elevated expression of cell proliferation marker protein in the osteogenic front of calvaria of MS-275–treated newborn mice (Fig. 13B). Moreover, administration of a low dose of MS-275 stimulated cell growth of primary osteoblasts (Fig. 13C). These observations corroborate our speculation that MS-275 promotes cell proliferation, thereby accelerating the process of suture closure. These findings supported the RNA-seq

results indicating that MS-275 exerts a positive effect on bone formation. Moreover, by selecting genes with high significance ($P<0.05$, 95% confidence) from among 118 genes involved in apoptotic processes, including those involved in cell death and DNA damage response, we found that MS-275 exerted an inhibitory effect on apoptosis. This is reasonable because this observation corresponds to the observed promotion of proliferation; moreover, it is consistent with previous reports that elevation of apoptosis during development leads to delayed suture closure and acrania-like craniofacial deformities [58,59]. Collectively, these data indicate that the Runx2 stimulating effect of MS-275 can increase osteoprogenitor cell number in suture space by stimulating proliferation and stimulate further differentiation of these cells in *Runx2*$^{+/-}$ mouse calvarial cells and tissue.

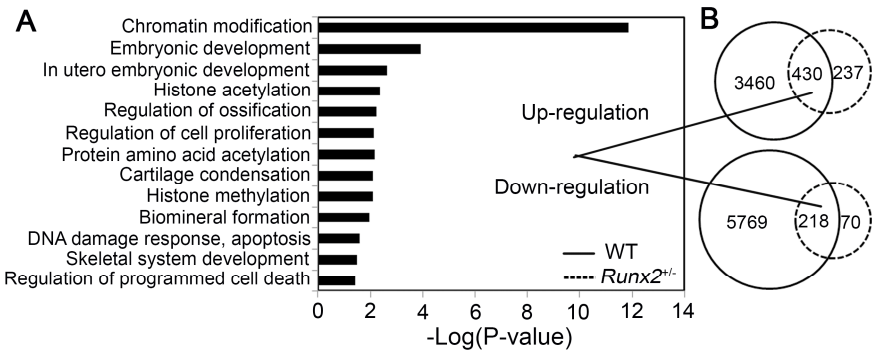

Fig. 11. Next Generation Sequencing (NGS) analysis shows effects of MS-275 on osteoblast proliferation and differentiation. (**A**) Gene ontology (GO) pathway analysis of E17.5 mouse calvaria of both genotypes that were injected *in utero* with MS-275, in comparison with vehicle-injected fetal calvaria. GO biological process are depicted according to p-values. (**B**) Venn diagrams of genes up- and down-regulated following MS-275 treatment in WT (solid line) and *Runx2*$^{+/-}$ (dotted lined) calvaria. Regulated genes from (**A**) were counted and classified.

Table 5. Genes differentially regulated in calvarial bones from WT and *Runx2*$^{+/-}$ mice.

Gene Ontology (BP)	Gene symbol	WT MS / WT veh	*P*-Value	Het veh/ WT veh	*P*-value	Het MS/ Het veh	*P*-value	Het MS/ WT veh	*P*-value
Osteoblast differentiation & Bone development (GO0030278, GO0001502, GO0031214, GO0001501)	Bglap	5.47	0.001765**	1.07	0.058695	3.96	0.028163*	5.03	0.017623*
	Bglap2	5.33	0.001049**	0.66	0.10658	4.46	0.017984*	5.12	0.011772*
	Spp1	5.22	0.005409**	0.97	0.013661	4.33	0.015502*	5.3	0.010747*
	IBSP	4.41	0.011214*	0.3	0.74403	3.98	0.042445*	4.29	0.020973*
	Mgp	3.44	0.000187***	1.09	0.181009	2.79	0.042726*	3.88	0.00457**
	Chrdl1	2.79	0.001786**	1.03	0.06995	2.01	0.018468*	3.04	0.000687***
	Sp7	2.46	0.022407*	0.48	0.461864	0.56	0.325346	1.04	0.105766
	Alpl	2.38	0.012848*	0.42	0.484484	0.59	0.289332	1	0.066842
	Ostn	1.71	0.004562**	0.6	0.180902	2.21	0.017966*	2.82	0.000191***
	Runx2	1.42	0.008117**	0.47	0.040506*	0.42	0.082761	0.9	0.015219*
Proliferation (GO0008284, GO0042127)	Timp1	4.52	0.008687**	0.9	0.166373	3.75	0.020553*	4.65	0.019854*
	Clec11a	3.24	0.001439**	0.76	0.019177*	1.83	0.001336**	2.59	0.002098**
	Npm1	2.1	0.024798*	0.43	0.341367	1.99	0.043799*	2.42	0.01656*
	Rpl29	2.05	0.009792**	0.52	0.343706	1.81	0.061645	2.33	0.016414*
	Pmp22	1.65	0.001248**	0.44	0.057726	1.84	0.005173**	2.38	0.00192**
	Pcna	1.32	0.021318*	0.4	0.312042	1.28	0.129808	1.67	0.066939
	Ctnnb1	1.29	0.01308*	0.03	0.807585	0.96	0.007803**	0.99	0.002842**
	Mki67	0.28	0.25916	0.12	0.598139	0.56	0.04639*	0.68	0.042468*
Apoptosis (GO0042771)	Trp63	-5	0.006082**	-0.28	0.742582	-4.98	0.032375*	-5.27	0.017545*
	Bcl2l14	-4.24	0.005475**	-0.56	0.403791	-3.71	0.349202	-4.28	0.292615
	Faim2	-3.61	0.023135*	-1.33	0.214338	-1.95	0.111423	-3.27	0.009371**
	Fasl	-2.99	0.005856**	-0.16	0.83417	-2.84	0.044109*	-2.99	0.005856**
	Perp	-2.63	0.047413*	-0.02	0.968812	-2.4	0.005865**	-2.42	0.044776*
	Atf6b	-0.93	0.016225*	-0.36	0.287011	-1.01	0.060303	-1.37	0.009333**

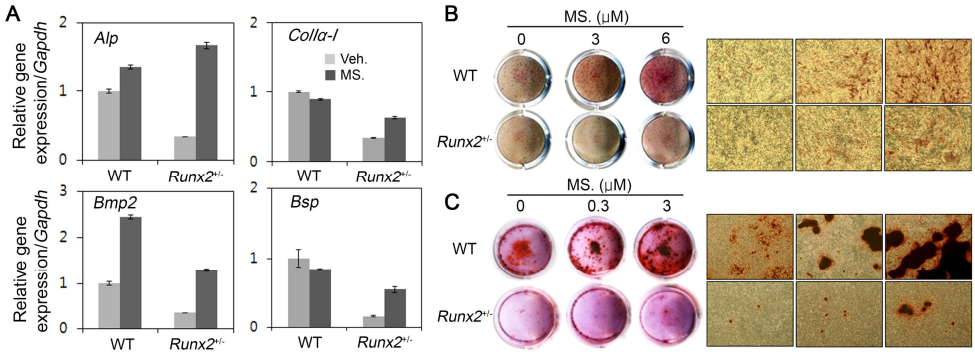

Fig. 12. MS-275 induces osteoblast differentiation. (**A**) Relative expression of bone marker genes was assessed based on qPCR analysis from E17.5 mouse calvaria to validate the RNA-seq results. The level of osteoblast differentiation was estimated by (**B**) ALP staining and (**C**) Alizarin red S staining assay. Primary cells were cultured in osteogenic media after 24 hr culture with the indicated concentration of MS-275. Stained areas are magnified beside the panel. All experiments were performed in triplicate. Veh.= Vehicle, MS.= MS-275. *P<0.05, **P<0.01, ***P<0.001, Student's *t*-test.

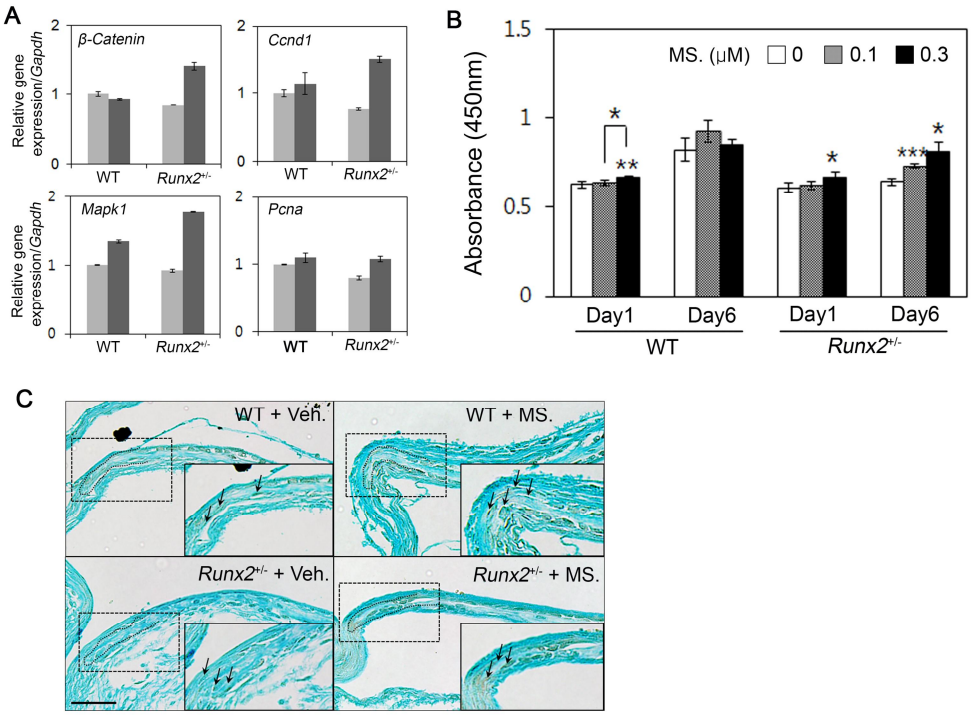

Fig. 13. MS-275 stimulates cell proliferation (**A**) Relative expression of proliferation marker genes from E17.5 mouse calvaria to validate the RNA-seq results. (**B**) Ki-67, a marker of proliferation, was detected at the osteogenic front region of P0 mouse calvaria (Scale bar, 50 μm). The region of calvarial bone is marked with dotted line. The osteogenic front region is magnified in box inset. Arrows indicate positively stained cells. (**C**) Proliferation assay results from primary mouse calvarial cells. Following treatment with different doses of MS-275 for 24 hr, proliferation rates were evaluated after additional culture for 1 day and 6 days. All experiments were performed in triplicate. Veh.= Vehicle, MS.= MS-275. *P<0.05, **P<0.01, ***P<0.001, Student's *t*-test.

Discussion

Previously, it was suggested that a threshold level of RUNX2 is required for the normal skeletal development [39], and that RUNX2 is deficient in human CCD patients and *Runx2*$^{+/-}$ mice [11]. In this study, we tested the hypothesis that restoration of Runx2 activity by MS-275 treatment could prevent development of CCD-like phenotypes in *Runx2*$^{+/-}$ mice. Indeed, our results show that fetal administration of MS-275 during early skeletal development rescued *Runx2*$^{+/-}$ mice from CCD-like phenotypes related to development of the cranial suture, mandible, and clavicle (Fig. 1). Rescuing CCD-like phenotypes could be more effective when we adjust the initiation stage, dosage and frequency of drug treatment with pharmacokinetic analysis. However, since we administrated chemicals in utero, there was a limitation of using *Runx2*$^{+/-}$ mice for this study; we could not rule out the maternal effects on the embryos during pregnancy. To overcome this limitation, we showed double fluorescence labeling assay accompanied with organ culture system. In this study, we showed MS-275 exerted a much stronger effect on intramembranous rather than endochondral bone formation. In contrast to the prominent effect in flat bones, long bone development was neither significantly perturbed by *Runx2* deficiency nor significantly improved by MS-275 (Fig. 3). Clavicles develop by both endochondral (lateral part) and intramembranous (medial part) bone formation processes[41]. In hypoplastic clavicles, the medial part is usually missing. We found that MS-275 treatment primarily restored the medial part of the clavicles in *Runx2*$^{+/-}$ mice, indicating that intramembranous bone

formation is more sensitive to the restoration of Runx2 function by MS275 treatment (Fig. 2). Compared to other membranous bones like calvaria and mandible, MS-275 did not restore clavicle formation that markedly. This may be because clavicles are among the earliest bones to develop [60], whereas we initiated MS-275 administration at 14.5 d.p.c., potentially too late to recover clavicles. Thus, earlier administration might be preferable for this purpose. These results demonstrated that genetic insufficiency of a gene due to a single-allele loss-of-function mutation can be rescued by increasing protein activity or stability with specific modulators. This approach could also be applied to the treatment of other single-gene genetic disorders.

Next, we addressed the mechanism underlying the effects of MS-275 on CCD-like phenotypes. First, we are suggesting MS-275 has a role in Runx2 post-translational modification because it can acetylate Runx2, generating the functionally activated form. As expected, acetylated Runx2 was stabilized and spared from degradation, and both its abundance and transactivating activity increased (Fig. 5-7). Nonetheless, it remains possible that the level of Runx2 protein was indirectly elevated resulting from an increase in *Runx2* mRNA expression in response to MS-275 treatment, as shown in Fig. 9A. Therefore, to rule out this background, we carried out tag-detection system in immune blot after overexpression of MYC-tagged-Runx2 (Fig. 5D). Previous study also demonstrated by using overexpression of tagged-Runx2 system that HDAC deacetylates Runx2 and HDIs increases its acetylation [14]. These results indicate

that MS-275 can enhance Runx2 protein activity in the absence of transcriptional upregulation of endogenous *Runx2*. Second, MS-275 can modify the epigenetic landscape. Specifically, the drug decreased the methylation level of the CpG island in the *Runx2* promoter 2, thereby stimulating *Runx2* expression. This observation is consistent with previous reports that MS-275 promotes both histone acetylation (by inhibiting HDAC) and CpG demethylation (by repressing DNA methyltransferase) [(61)]. In aspects of histone modification, our results of ChIP assay and immune blot assay were also comparable with previous study, which demonstrated marked histone modification dynamics during osteoblast differentiation (Fig. 9B, Fig. 10). In the process of osteogenesis, promoter region of *Runx2* experienced elevated H3 and H4 acetylation and reduced H3K9, H3K27 methylation whereas global level of those hall marks were not changed [(48)]. Collectively, these changes promote *Runx2* transcription (Fig. 9A). Together with post-translational modification of Runx2 protein, the positive effect on transcription may be sufficient to reach the threshold Runx2 level required to overcome genetic haploinsufficiency.

What, then, is the functional consequence of Runx2 activation in the early skeletogenesis? Our RNA-seq results indicated that MS-275 strongly stimulated the expression of osteoblast marker genes, as was well known from previous studies [(27)]. In addition, we observed significant upregulation of proliferation-related genes and downregulation of apoptosis-related genes (Fig. 11, Table. 5). Previously, we showed that many HDIs can stimulate Runx2 activity [(14)]. These observations are correlated with study of *Schroeder* and colleague. They showed

increased ALP activity in calvarial tissue cultured media after MS-275 treatment and suggested MS-275 has a role in enhancing Runx2 transcriptional activity [28]. In this study, we found that MS-275 has a clear therapeutic effect on CCD. This might be explained in any of several ways. First, the differences in the effects of MS-275 may be due to its distinct specificities on HDAC1 and 3. MS-275 preferentially inhibits HDAC1 and 3 with IC50 of 0.51 and 1.7μM correspondingly. Previous reports showed that HDAC1 binds to promoters of the bone marker genes osterix and osteocalcin to repress their expression [62]. In addition, HDAC3, a well-known transcriptional co-repressor of Runx2, works as a negative regulator of lineage-committed osteoblasts by binding to NFATc1, Zfp521, TCF, and Runx2 [25]. Collectively, these facts could explain, at least in part, the successful therapeutic effect of the class I–specific inhibitor MS-275. Second, marked stimulating activity toward cell proliferation might cause distinct CCD recovery effects. MS-275 presented effective stimulation on expression of proliferation marker genes and proliferation process (Fig. 13, Table 5). In the previous study, we found that MS-275 stimulates bone formation by interaction with Dhx36 [27], also known that it has critical roles in process of cell proliferation [63]. Therefore, we deduced that Dhx36-mediated signaling might be participated in highly triggered cell proliferative activity through MS-275 administration. Considering significance of proliferation of osteoblast progenitor cells in calvarial suture region during development [55], it could be the critical distinction of MS-275 treatment toward CCD.

Based on our findings and previous reports we conclude that the combined functions of MS-275 are responsible for the effects; Runx2 activation through PTM and transcriptional activation of *Runx2* via epigenetic regulation (Fig. 14). To reach comparable therapeutic effect with a single mechanism, just by PTM or by epigenetics, the therapeutic dosage might be increased higher to generate more side effects. The dosage of MS-275 in this study is much less than one tenth of other experiments [(64)] and the litter number of MS-275 treated mice was comparable that of untreated control. These results indicate combination of both mechanisms synergized to enhance Runx2 specific activity of the agent with a lower dose. In addition, the enhanced Runx2 function by MS-275 stimulates osteoblast proliferation and differentiation processes. However, we must be cautious when interpreting the relationship between cell proliferation and MS-275 since it also has anti-proliferative effects and apoptosis-inductive properties as an anti-cancer reagent. However, many studies show that the effect of HDIs including MS-275 on cell proliferation is concentration-dependent: in general, they promote proliferation at low dose but inhibit growth at high dose [(28)]. Although we could not observe any skeletal malformation as a side effect of HDI administration, some kinds of HDIs, valproic acid and trichostatin A (TSA) for instance, were reported as teratogenic reagents for developing mouse skeletons causing embryonic skeletal malformation including vertebral or rib fusions at high dose administrations [(65)]. Thus, more extensive- toxicological study would be required to apply HDIs in clinical field.

As regulation of *Runx2* activity is of tremendous interest from the standpoint of developing therapeutic agents against skeletal diseases, our findings have important medical implications. Notably, we demonstrated that MS-275 could compensate for genetic insufficiency of *Runx2* in *Runx2*$^{+/-}$ mice. Therefore, the use of this drug thus represents a promising chemo-preventive strategy for a genetic disease, CCD, especially if it can be diagnosed before birth. MS-275 also holds tremendous potential as a therapeutic agent for diseases involving the *Runx2* gene, including many bone disorders. Thus, our results provide a novel experimental and theoretical basis for developing therapeutic agents against CCD and other skeletal diseases.

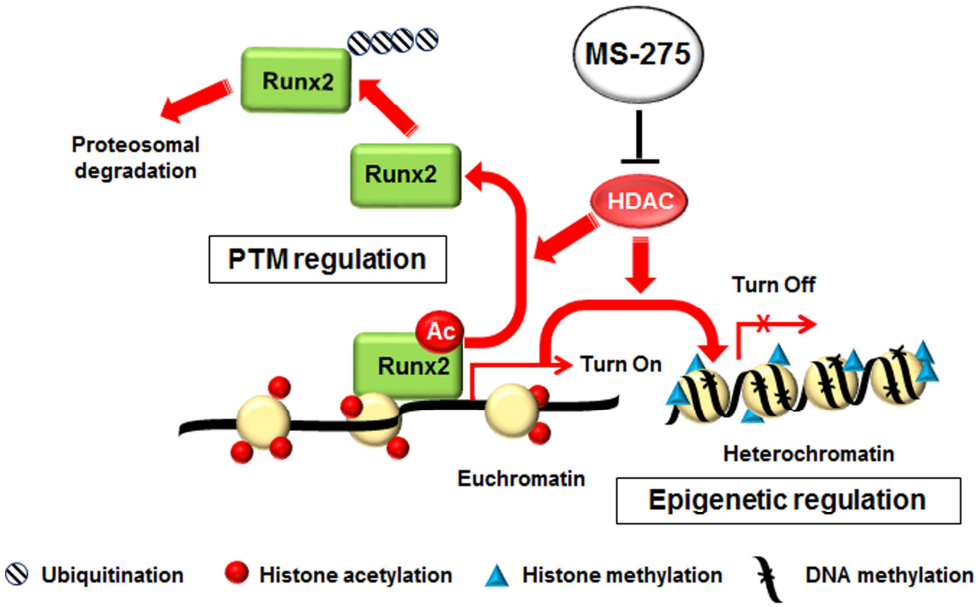

Fig. 14. Mechanism of *Runx2* activation by MS-275. MS-275 regulates *Runx2* expression via two mechanisms. 1) Stabilization of Runx2 protein through post-translational modification (PTM), which induces Runx2 acetylation and protects Runx2 from ubiquitination. 2) Epigenetic activation of the *Runx2* promoter region via alteration of the epigenetic landscape. MS-275 activates the *Runx2* promoter by modifying chromatin structure from heterochromatin to euchromatin by increasing histone acetylation and decreasing CpG and histone methylation. HAT= Histone Acetyl Transferase, Ac= Acetylation.

IV. Part II.

RNA-seq. data analysis identifies MS-275 as an activator of osteoblast differentiation of *Runx2*$^{+/-}$ mouse calvarial cells

Abstract

The genetic mechanisms regulating osteoblasts differentiation is still not fully understood. Previously, we found that Histone deacetylase inhibitor (HDI), MS-275 rescues CCD phenotypes of *Runx2*$^{+/-}$mice and delayed osteoblast differentiation of *Runx2*$^{+/-}$ mouse calvarial cells. Herein, we performed an RNA-seq on WT and *Runx2*$^{+/-}$ mouse calvarial cells either with or without MS-275 treatment and identified a Runx2 specific gene expression signatures and MS-275 dependent changes on biological processes. Furthermore, bioinformatics analysis on the RNA-seq. data identified a group of genes regulating cell proliferation and osteoblast maturation of which expressions were altered by *Runx2* haploinsufficiency and recovered after MS-275 treatment. Concordantly, these genes are consistent with our idea about the role of MS-275 since they are known to interact with Runx2 to regulate process of bone formation. Our study provide insight into the understanding of the correlation between the pathological consequence of *Runx2* deficiency and therapeutic effect of histone deacetylase inhibition through facilitating osteogenesis.

Introduction

During skeletal development, expressions of many genes are highly regulated and thus result in specific cell phenotypes depend on differentiation stage. The expression pattern of the genes changed when the intracellular environment changes. The altered gene expression means a change in cell function, which changes the cell fate.

Bone formation is conducted by two kinds of development processes; Endochondral ossification and intramembranous bone formation. Both processes require differentiation of mesenchymal stem cells (MSCs) into chondrocytes (in case of endochondral bone formation) and/or osteoblasts. Cells in endochondral bone development would be involved in mesenchymal condensation to form cartilage anlagen. To occur these events, several chondrocyte-specific genes are expressed including *Sox9*, *Gli3*, and *Hoxa13*. *Sox9* plays a crucial role in cartilage development by permitting transcript of aggrecan (*Acan*), collagen type II, collagen type IX, and cartilage oligomeric protein (*Comp*). According to these gene expressions, chondrocytes in the growth plate proliferate and undergo extracellular matrix (ECM) deposition and hypertrophy to promote bone lengthening. At the late stage of the endochondral bone formation, hypertrophic chondrocytes down-regulate expression of collagen type II and start to secrete collagen type X, and ossify the ECM with expression of *Runx2*, *Osterix*, *Msx2*. As maturation progresses, hypertrophic chondrocytes stimuli production of vascular endothelial growth factor (*Vegf*), which trigger vascularization and metalloproteinases (*Mmps*), which

support ossified cartilage matrix turnover. Through these series of cellular maturation processes develop into long bones comprise the appendicular skeleton, vertebrae, facial bones, and the lateral parts of clavicles.

On the other hand, cells undergo intramembranous ossification, differentiate into osteoprogenitor cells after aggregation of mesenchymal cells into condensation centers. In this period, cells permit transcription of *Bmp2*, *Bmp4*, several Wnt ligands, *β-catenin*, and *Fgf2* for proliferation. Subsequently differentiated into pre-osteoblasts and matured to osteoblasts that act as a critical player in osteogenesis. Those osteogenic cells generally express collagen type I, osteopontin (*Opn*), alkaline phosphatase (*Alp*), osterix (*Osx*), Dlx5 and osteocalcin (*Oc*) to secrete ECM components, osteoids, and uncalcified matrix, which ultimately calcifies as mineral slats are deposited on it, thereby forming intramembranous bone. Throughout these developmental steps, intramembranous ossification gives rise to the flat bones constitutes the cranium and medial clavicles.

Expression of genes during early stage of bone formation is mostly influenced by Runx2, the master transcription factor in osteogenesis. Runx2 plays a role in controlling a complex gene-transcription system during osteoblast differentiation. It upregulates the expression genes involved in osteoblast lineage-specific group such as *Osx, Oc*, and *Bsp*, and represses the non-osteoblast genes including MyoD (myogenic differentiation), and PPAR γ (peroxisome proliferator-activated receptor gamma) which are essential for myogenesis and adipogenesis, respectively. In addition, recently, transcriptional regulation by chromatin

remodeling has become as important mechanism as that by transcription factors. It has been reported in numerous studies that modulation of epigenetic landscape could affect key transcriptional factors to determining gene expression and differentiation of mesenchymal stem cells. Epigenetic regulation refers to a change in chromatin structure, which is derived by the modification of histone proteins includes acetylation, methylation and phosphorylation. Epigenetic modulation is able to induce heritable changes in gene expression via modification of chromosomal structure other than alteration of the DNA sequence. Acetylation or deacetylation of histone has an important responsibility in the process of gene transcription which is regulated by a balance of the enzymatic activity of histone acetyltransferase (HAT) and histone deacetylase (HDAC). Dynamic equilibrium of the two distinct enzymatic activities are critical for the activation of transcription and regulation of gene expression in eukaryotic cells.

A number of studies investigated the biological role of chemical compound, which inhibit HDAC activity for their possible therapeutic effects. HDAC Inhibitors (HDIs) transform histone to hyper-acetylated form, which result s in the relaxation of the DNA structure, which in turn activates the expression of specific genes. Previously, we demonstrated that Class I HDI, MS-275, recovered hypoplastic bone formation of *Runx2*$^{+/-}$ mice and enhanced osteoblast differentiation in *Runx2*$^{+/-}$ mouse calvarial cells. Moreover, *Dudakovic* et al. revealed that HDI stimulated osteoblast differentiation by increasing Runx2 activity. These studies have highlighted the regulatory role of HDI towards Runx2

transacting activity and *Runx2* transcription. However, the entire genetic scope of Runx2 haploinsufficiency and MS-275 administration remains largely unknown. Herein, we have characterized the gene expression profile by RNA-sequencing in WT and *Runx2*$^{+/-}$ mouse calvarial cells which were cultured with or without MS-275 treatment. Analysis of this data indicated that dynamic changes in the gene expression pattern due to the genetic background and/or chemical treatment are related to the biological characteristics of cells and it would be an important tool to explain the biological phenomenon.

Results

Differentially expressed genes in each cellular context were discovered by RNA-sequencing.

Although Runx2 is a well-known central regulator of bone formation and MS-275 have also reported as activator of osteoblast differentiation, only a small number of target genes have been identified. To examine genome-wide gene expression pattern according to the physiological environment, Runx2-deficiency and/or chemical treatment, we carried out RNA- sequencing (RNA-seq.) technique. There were 22.37 million short reads and 28,957 references of genes to analyze RNA expression profile. After quality filtering, approximately 8,800 differentially expressed genes were detected in each group. The genes were filtered using P-value < 0.05 threshold that produced 441, 2,486, 1,940, and 1,273 differential gene sets for WT vs WT with MS-275 treatment, WT vs *Runx2*$^{+/-}$ both with vehicle treatment, *Runx2*$^{+/-}$ vs *Runx2*$^{+/-}$ with MS-275 treatment, and WT vs *Runx2*$^{+/-}$ both with MS-275 treatment, respectively. Each gene was categorized according to its fold change value (Table 6). Heat-map analysis revealed that there are many genes that are regulated expression in various manner according to each context of cells. Therefore, we clustered genes based on the expression pattern in the genetic background and physiological context (Fig 15).

Table 6. RNA-sequencing analysis of primary mouse calvarial cells.

Specification	WT vs WT+MS.	WT vs Runx2$^{+/-}$	Runx2$^{+/-}$ vs Runx2$^{+/-}$ + MS.	WT + MS. vs *Runx2*$^{+/-}$ + MS.
Total number of genes	28,957	28,957	28,957	28,957
Detected gene expression	8,211	8,140	8,119	7,580
P-value < 0.05	441	2,486	1,940	1,273
2 - 5 fold upregulated	119	196	195	141
5 - 10 fold upregulated	35	12	13	19
> 10 fold upregulated	65	2	5	28
2 - 5 fold downregulated	65	34	21	60
5 -10 fold downregulated	18	147	0	3
> 10 fold downregulated	9	1	0	0

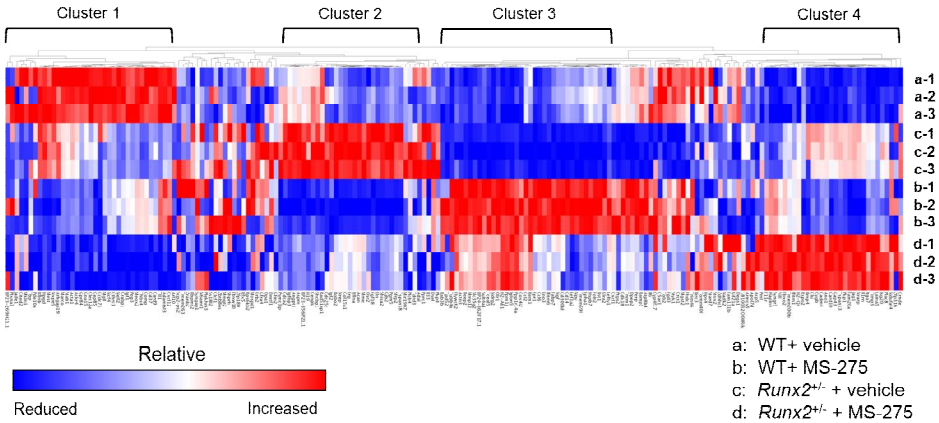

Fig 15. Heat-map analysis of the normalized expression level of the 194 DEGs for each group. 194 gene expression patterens for WT and *Runx2*$^{+/-}$ genotype mouse calvarial cells cultured with or without MS-275 treatment. Genes were clustered according to their distinct expression pattern. Gene expression level was measured by RNA-seq. analysis with value expressed as Reads Per Killobase of transcript per Million mapped reads (RPKM). Increased and decreased levels of gene expression are shown in blue (decreased) and red (increased) color, respectively.

***Runx2* haploinsufficiency causes dynamic alteration of gene expression.**

As reported previously, Runx2 heterozygous null mice showed phenotypes of Cleidocranial dysplasia and *Runx2*$^{+/-}$ cells exhibited delayed osteoblast differentiation. To gain insight into molecular properties of *Runx2*, we constructed scatter plot to recognize the expression patterns of each comparative groups. Firstly we set the value of $\log_2$(*Runx2*$^{+/-}$ MS/*Runx2*$^{+/-}$ veh.) as an X-axis to measure the expression differences of MS-275 treatment toward vehicle treatment in *Runx2*$^{+/-}$ cells and the $\log_2$(*Runx2*$^{+/-}$ veh./WT veh.) as an Y-axis to compare between WT and *Runx2*$^{+/-}$ cells in vehicle treated group. Analysis of the RNA expression plot revealed that 4399 genes are down-regulated in WT versus *Runx2*$^{+/-}$ and 4440 genes are up-regulated (Fig. 16A). We deduced that these differentially expressed genes could provide the clue of pathological effects of *Runx2*-deficiency which cause imperfect differentiation into osteoblasts. To identify biological processes changed by *Runx2* haploinsufficiency, we subjected the differentially expressed genes (DEGs) to gene ontology (GO) analysis of biological process. GO term analysis showed that genes down-regulated by *Runx2*-deficiency are comprised in cell activation, angiogenesis, cell communication and bone formation-related processes such as ossification, ossification, embryonic skeletal system development. Up-regulated genes in *Runx2*$^{+/-}$ samples were enriched for processes associated angiogenesis, chromosome segregation, cell signaling and osteogenesis-related processes including osteoblast differentiation and embryonic skeletal system development (Fig 16B). These results show that how *Runx2*

haploinsufficiency influences general gene expression and biological processes.

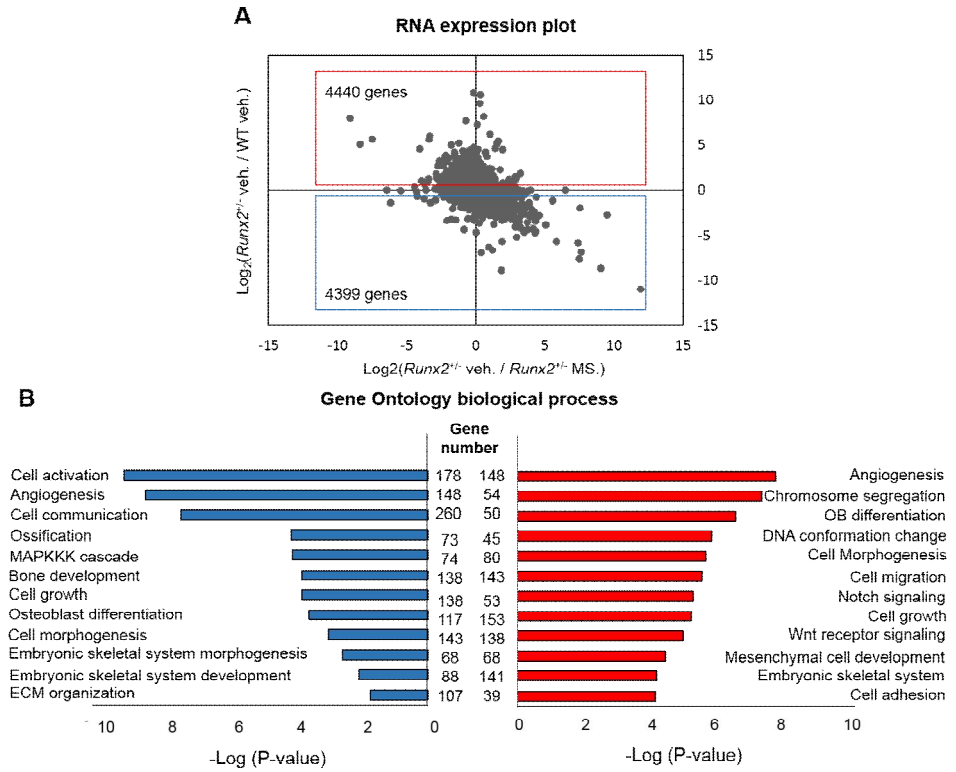

Fig. 16. The pattern of gene expression and biological process are altered by *Runx2* haploinsufficiency in mouse calvarial cells. (**A**) Scatter plot depicting the correlation between relative gene expression value of *Runx2*$^{+/-}$ calvarial cells with vehicle treatment versus *Runx2*$^{+/-}$ cells with MS-275 (X-axis) and *Runx2*$^{+/-}$ cells with vehicle versus WT vehicle (Y-axis). (**B**) Analysis of gene ontology of biological functions for down-regulated (blue-colored bar) and upregulated (red-colored bar) genes from *Runx2*$^{+/-}$ with vehicle versus WT with vehicle RNA-seq. data sets. The value of $\log_2$(fold change) is used to create 2D plots.

MS-275 treatment have affected gene expression pattern on *Runx2*$^{+/-}$ mouse calvarial cells

Since we eager to explore the phenomenon that altered expression of the genes in disease model were restored through HDAC inhibition, we focused on quadrant II and quadrant IV of expression plot in Fig. 16. Analysis of gene sets in these quadrant we were able to unravel the biological relevance of the MS-275 treatment and *Runx2* haploinsufficiency. 336 Genes in the quadrant II, their expression was increased in *Runx2*$^{+/-}$ and decreased after MS-275 treatment. On the other hand, 381 genes in quadrant IV, their expression was reduced in *Runx2*$^{+/-}$ cells and rise in MS-275 treated group (Fig. 17A). To further explore the correlation between genes in each quadrant and biological process, we performed functional annotation using Gene-Set Enrichment Analysis (GSEA). Analysis of Gene Ontology (GO) terms which associated with significantly changed genes were indicated in Fig. 17B. Genes in quadrant II yielded GO terms of proliferation, bone development, and ossification. Gene in quadrant IV associated GO terms of immune response, angiogenesis, bone development, and biomineral formation.

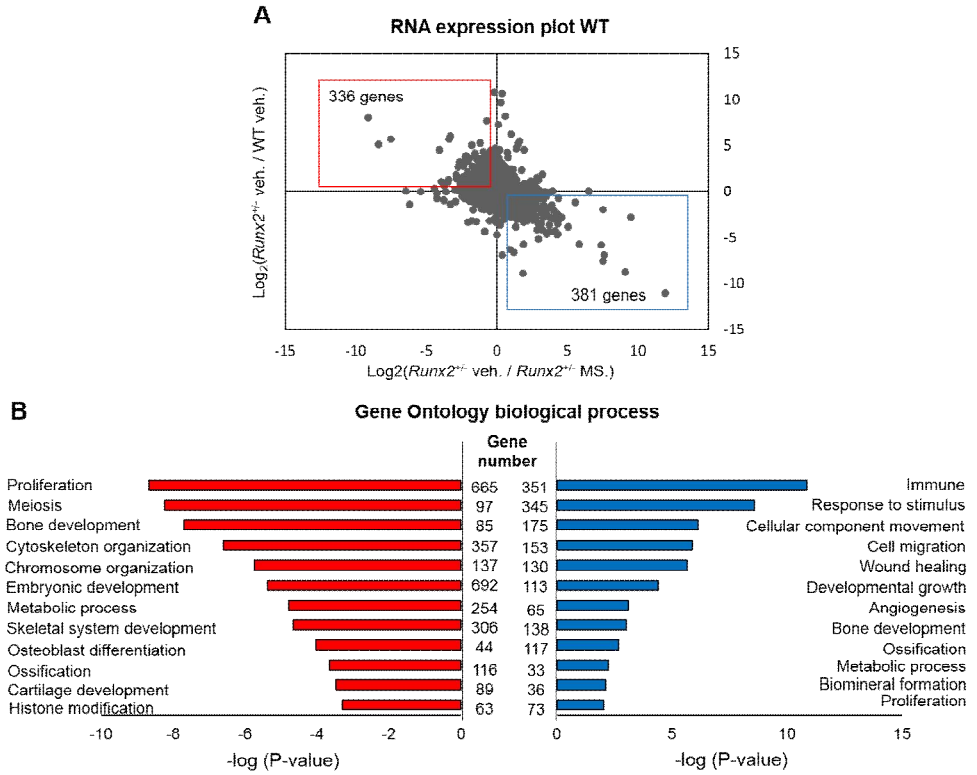

Fig. 17. Treatment of MS-275 modifies gene expression pattern in *Runx2*$^{+/-}$ mouse calvarial cells. (**A**) Expression plot of RNA-seq. results. Relative gene expression value of *Runx2*$^{+/-}$ calvarial cells with vehicle treatment versus *Runx2*$^{+/-}$ cells with MS-275 (X-axis) is plotted on the *Runx2*$^{+/-}$ cells with vehicle versus WT vehicle (Y-axis) site of correspond gene. (**B**) Analysis of gene ontology of biological functions for downregulated (blue-colored bar) and upregulated (red-colored bar) genes from *Runx2*$^{+/-}$ with vehicle versus WT with vehicle RNA-seq. data sets. The value of $\log_2$(fold change) is used to create 2D plots.

Genes showing significant patterns in *Runx2* haplodeficiency and by MS-275 treatment could be a therapeutic marker of cleidocranial dysplasia.

A number of enriched GO terms were related to osteogenesis and skeletal development (Fig. 17B). As we investigated the genetic mechanism that delayed osteogenesis was restored through MS-275 treatment, narrow down to target associated with bone formation which overlapped GO term of genes involved quadrant II and quadrant IV in RNA expression plot (Fig. 17). We detected 7 bone development-related genes from quadrant II; *Acan, Fbn2, Sfrp2, Col11αI, Igfbp3, Col2αI, Col8αII*, 8 genes from quadrant IV; *Junb, Ecm1, Csf1, Msx2, Acp5, Ptgs2, Grem1, Cd24a* (Fig. 18A, B, Table. 7). Among those 15 candidate genes, we selected 4 of the most significant genes, *Acan, Fbn2, Ifgbp3, and Csf1* according to relative P-values (Fig 18C). In addition, we examined the recovery levels of candidate genes how closely the genes recovered to the normal trait after MS-275 treatment (Fig. 18D). To validate the actual gene expression level of the RNA samples correspond to the RNA-seq. results, we carried out quantitative real-time PCR (Fig. 18E). We have confirmed that the RNA expression level of all target genes is consistent with the patterns seen in data of RNA-seq. analysis.

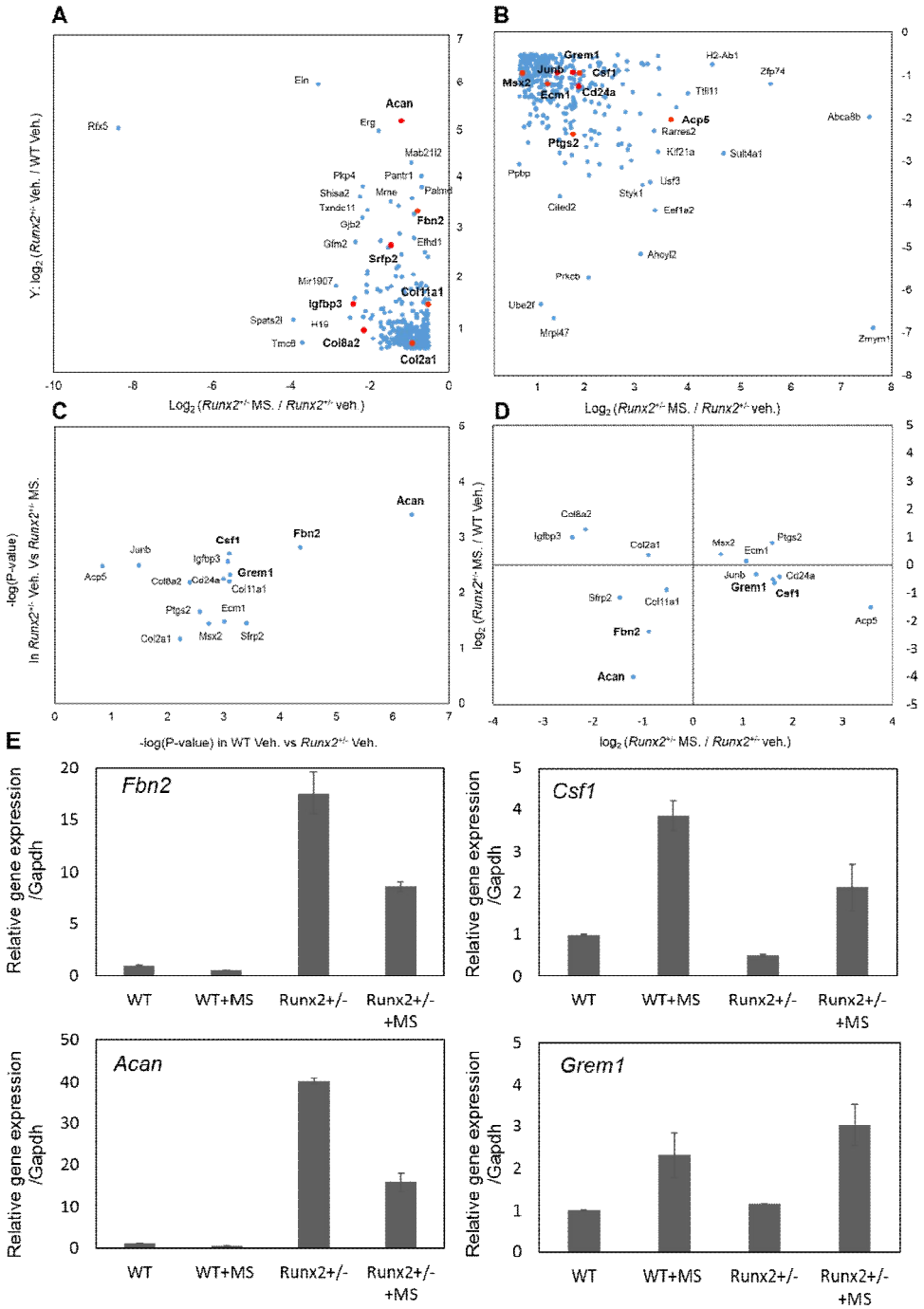
A
Y: log2 (Runx2+/- Veh. / WT Veh.)
Log2 (Runx2+/- MS. / Runx2+/- veh.)
Acan
Fbn2
Srfp2
Col11a1
Igfbp3
Col8a2
Col2a1
B
Log2 (Runx2+/- MS. / Runx2+/- veh.)
Grem1
Junb
Csf1
Msx2
Ecm1
Cd24a
Acp5
Ptgs2
C
-log(P-value) in Runx2+/- Veh. Vs Runx2+/- MS.
-log(P-value) in WT Veh. vs Runx2+/- Veh.
D
log2 (Runx2+/- MS. / Runx2+/- Veh.)
log2 (Runx2+/- MS. / Runx2+/- veh.)
E
Fbn2
Csf1
Acan
Grem1
Relative gene expression /Gapdh
WT
WT+MS
Runx2+/-
Runx2+/- +MS

Fig. 18. Target gene selection using RNA expression plot and P-value. (**A, B**) Expression plot of RNA-seq. results. Relative gene expression value of *Runx2*$^{+/-}$ calvarial cells with vehicle treatment versus *Runx2*$^{+/-}$ cells with MS-275 (X-axis) is plotted on the *Runx2*$^{+/-}$ cells with vehicle versus WT vehicle (Y-axis) site of correspond gene. Genes expressed higher level in *Runx2*$^{+/-}$ cells than WT and decreased with MS-275 plotted on graph (**A**). Genes exhibited reduced expression pattern in *Runx2*$^{+/-}$ and increased with MS-275 treatment were plotted on graph (**B**). (**C**) The 15 candidates of target genes are plotted according to their relative p-values. (**D**) RNA expression plot with X-axis of $\log_2$(*Runx2*$^{+/-}$ MS-275 / *Runx2*$^{+/-}$ vehicle) and Y-axis of $\log_2$(*Runx2*$^{+/-}$ MS-275 /WT vehicle) which can show recovery levels of gene expression in *Runx2*$^{+/-}$ cells with MS-275 treatment. (**E**) Expression patterns of each target gene were validated by quantitative real-time PCR.

Table 7. Differential expression levels of target genes in mouse calvarial cells.

Genes	WT veh. vs *Runx2*$^{+/-}$ veh.	p-value	q-value	*Runx2*$^{+/-}$ veh. vs *Runx2*$^{+/-}$ MS.	p-value	q-value
Acan	11.1744329	4.65E-07	0.001892	0.455231286	0.000384	0.051473
Fbn2	9.025270758	4.40E-05	0.008946	0.598631579	0.001549	0.061684
Sfrp2	6.106864869	0.000395	0.015497	0.569015007	0.035411	0.172115
Col11a1	2.599769388	0.000801	0.019357	0.748048169	0.006383	0.088799
Igfbp3	2.741899084	0.000848	0.019624	0.227494826	0.002749	0.069889
Col2a1	1.570133121	0.006057	0.047308	0.546726557	0.068149	0.239512
Col8a2	1.840067906	0.00407	0.038739	0.313295583	0.006669	0.090191
Junb	0.547682533	0.032842	0.125231	3.94599849	0.00319	0.072944
Ecm1	0.482472949	0.000974	0.020287	2.069059038	0.033459	0.168035
Csf1	0.564773069	0.000791	0.01922	3.38933912	0.001989	0.065489
Msx2	0.615819135	0.001849	0.027167	1.677436818	0.036422	0.174623
Acp5	0.510788272	0.145461	0.317653	10.96126466	0.003288	0.073349
Ptgs2	0.195628973	0.0027	0.032745	3.481745272	0.02182	0.138157
Grem1	0.452214895	0.000777	0.018983	2.630160595	0.004725	0.080111
Cd24a	0.435330391	0.001007	0.020684	2.675680921	0.005688	0.084185

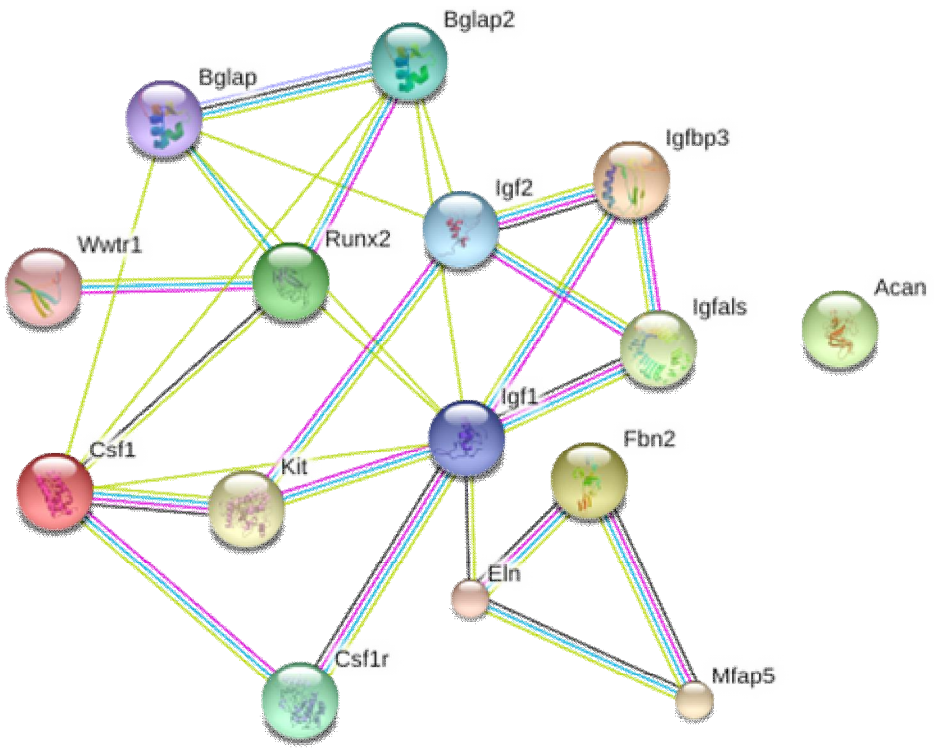

Fig. 19. The string diagram shows the predicted protein-protein interactions of the 5 queries (Runx2, Acan, Csf1, Fbn2, and Igfbp3) of differentially expressed genes. Colored nodes in string diagram represent query proteins and their reported interactions with multiple nodes. Edges represent protein–protein associations, and different colors of the edges represent different associations. The known interactions were found from curated databases (blue) or experimentally confirmed (purple); the predicted interactions were suggested by gene neighborhood (green), gene fusions (red), or gene co-occurrence (dark blue); and other protein–protein associations were suggested by text-mining (yellow–green), co-expression (black), or protein homology (gray).

Discussion

Through comprehensive gene expression analysis of mouse calvarial cells by RNA-seq., we describe pathological effect caused by *Runx2* haplodeficiency and physiological consequences of HDAC inhibition on osteoblast. Genes cluster into expression pattern according to *Runx2* haploinsufficiency and MS-275 treatment related with broad range of biological function including angiogenesis, cell proliferation, ossification, and skeletal development. These results reflect that importance of Runx2 in osteogenesis and role of MS-275 as an activator toward osteoblast differentiation. Our study identified new Runx2-regulated genes (*Acan*, *Fbn2, Igfbp3* and *Csf1*) that found responsibility in delayed osteoblast differentiation in *Runx2*$^{+/-}$ cells, and more critically, shown possibility of being a marker for therapeutic efficacy because their altered expression patterns were recovered to those of WT level when MS-275 was treated.

The biological characteristics of the target genes are all related to the differentiation and maturation of osteoblasts. *Acan* (aggrecan) is a member belonging to the aggrecan/vesican proteoglycan family. An Acan act as major player in cartilage formation by constituting ECM and binding to calcium ion, which is also an important mechanism for the osteoblast maturation. Genetic defects in Acan is reported that it bring Osteochindritis Dissecans, Osteoarthritis and Spondyloepimetaphyseal dysplasia. *Fbn2* is a protein coding gene, encoding Fibrillin-2 which is structural components of extracellular calcium-binding microfibrills. Associated human diseases with *Fbn2* are Contractural

Arachnodactyly and Macular Degeneration which affect connective tissues and neuronal tissue respectively. The reason that defects in *Fbn2* causing these diseases might it involved in several signaling process such as phospholipase-c pathway and ERK signaling. Furthermore, fibrillin was known to be a factor controlling the maturation of osteoblast by regulating TGF-β and BMP signaling [66,67]. *Igfbp3* is one of the member of insulin-like growth factor binding protein (IGFBP) family. After formation of ternary complex of IGFBP protein, it circulates in the plasma and protects insulin-like growth factors (IGFs) from degradation. *Igfbp3* is known to be regulated by Runx2-dependent expression and is affected by FGF signaling during tooth development [68]. Lastly, *Csf1* (colony Stimulating Factor 1) is the gene encoding cytokine that regulates the function of macrophages. It is well-known factor as a regulator of osteoclast proliferation and differentiation, bone resorption and is also essential for normal skeletal development [69]. It is highly corresponding that the expression of genes related to osteoblast maturation changes with the haplodepletion of Runx2 and the treatment of potential therapeutic reagent, MS-275.

Through analysis of bioinformatics data, we could find a novel level of understanding of the compensated differentiation effect via HDAC inhibition which conducted previously [30]. Our study showed how the deficiency of *Runx2* affects the overall genes in cells and how those genes changed by MS-275 treatment. Some identified target genes which showing dynamically shifted expression could serve as a critical clue for understanding the pathological

mechanisms of the disease and the pharmacological effect of the MS-275 (Fig. 19). However, the results what we have identified are only a section of the biological event. Further experimental study is required to figure out whether significantly altered gene expressions were the cause or the result of the phenomenon. If we find a hidden link between the CCD and HDAC inhibition, the impact of our study investigating the genome-wide gene expression of primary mouse calvarial cells classified by genotype and HDI treatment sets an outline for understanding genetic insight of bone biology.

V. CONCLUSION

Runx2 is a key transcription factor in the osteogenesis and skeletal development. Controlling of bone formation has consistently been a major concern in the clinical field dealing skeletal diseases. In this study, we focused on mitigating phenotypes of CCD which caused by *Runx2* haploinsufficiency.

In the Part I, firstly I tried animal experiment to examine therapeutic effect of histone deacetylase inhibition by using MS-275. *In utero* administration of MS-275 showed a dramatic recovery effect on the *Runx2*$^{+/-}$ fetus. Subsequently, I found that MS-275 acetylates Runx2 transcription factor and increase its transactivating activity which ultimately leads to the promotion of osteoblast differentiation. Furthermore, I identified more that MS-275 could also stimulate *Runx2* transcription through epigenetic regulation. Based on these findings and previous studies I define that the combinated functions of MS-275 as follows; activates Runx2 protein through process of PTM and increase transcription of *Runx2* via mechanism of epigenetic regulation (Fig. 14). These functions of MS-275 stimulate biological procedures of osteoblast proliferation and differentiation.

In the Part II, I demonstrated that genome-wide gene expression is altered dynamically in the context of *Runx2* haploinsufficiency and MS-275 treatment. Although, it was well known that Runx2 regulate bone marker genes and MS-275 has characterized as activator of osteoblast differentiation, only a few genes were acknowledged. I get the data set of approximately 8,800 differentially expressed

genes (DEGs) by conducting RNA-seq. analysis. After clustering genes by expression pattern, I found 4 significant target genes (*Acan, Fbn2, Igfbp3*, and *Csf1*) which expression were altered in *Runx2*$^{+/-}$ cells and recovered in MS-275 treated cells. With this study, I suggest that these RNA-seq. data would provide genetic insight into *Runx2* haplodeficiency and histone deacetylase inhibition in mouse calvarial cells. The newly detected target genes could serve as a marker which able to verify therapeutic efficacy of MS-275 toward CCD.

Because regulation the activity of Runx2 is one of marvelous interest from current position of developing therapeutic drugs toward skeletal-related diseases, the findings from this study have significant medical implications. Remarkably, I exhibited that MS-275 is able to complement the disease phenotypes due to genetic deficiency of *Runx2* in both of *Runx2*$^{+/-}$ mice and *Runx2*$^{+/-}$ cells. In conclusion, the use of this agent thus works as an innovative chemo-preventive strategy for CCD. Furthermore, inferring though RNA-expression profile, MS-275 has great potential as a therapeutic agent for skeletal disorders not only associated with the *Runx2* gene but also other genes related skeletal disorder such as *Acan, Fbn2, Igfbp3* and *Csf1*. Therefore, my results support a novel theoretical insight and experimental basis for developing medical agents against CCD and other bone-related diseases.

VI. GENERAL REFERENCES

1. Quarles LD. Endocrine functions of bone in mineral metabolism regulation. The Journal of clinical investigation. Dec 2008;118(12):3820-8.
2. Lee NK, Sowa H, Hinoi E, Ferron M, Ahn JD, Confavreux C, et al. Endocrine regulation of energy metabolism by the skeleton. Cell. Aug 10 2007;130(3):456-69.
3. Yin T, Li L. The stem cell niches in bone. The Journal of clinical investigation. May 2006;116(5):1195-201.
4. Tuan RS. Biology of developmental and regenerative skeletogenesis. Clinical orthopaedics and related research. Oct 2004(427 Suppl):S105-17.
5. Hall BK, Miyake T. The membranous skeleton: the role of cell condensations in vertebrate skeletogenesis. Anatomy and embryology. Jul 1992;186(2):107-24.
6. Ogawa E, Maruyama M, Kagoshima H, Inuzuka M, Lu J, Satake M, et al. PEBP2/PEA2 represents a family of transcription factors homologous to the products of the Drosophila runt gene and the human AML1 gene. Proceedings of the National Academy of Sciences of the United States of America. Jul 15 1993;90(14):6859-63.
7. Lee DS, Choung HW, Kim HJ, Gronostajski RM, Yang YI, Ryoo HM, et al. NFI-C regulates osteoblast differentiation via control of osterix expression. Stem cells. Sep 2014;32(9):2467-79.

8. Lee MH, Kim YJ, Yoon WJ, Kim JI, Kim BG, Hwang YS, et al. Dlx5 specifically regulates Runx2 type II expression by binding to homeodomain-response elements in the Runx2 distal promoter. The Journal of biological chemistry. Oct 21 2005;280(42):35579-87.

9. Stein GS, Lian JB, van Wijnen AJ, Stein JL, Montecino M, Javed A, et al. Runx2 control of organization, assembly and activity of the regulatory machinery for skeletal gene expression. Oncogene. May 24 2004;23(24):4315-29.

10. Otto F, Thornell AP, Crompton T, Denzel A, Gilmour KC, Rosewell IR, et al. Cbfa1, a candidate gene for cleidocranial dysplasia syndrome, is essential for osteoblast differentiation and bone development. Cell. May 30 1997;89(5):765-71.

11. Mundlos S, Otto F, Mundlos C, Mulliken JB, Aylsworth AS, Albright S, et al. Mutations involving the transcription factor CBFA1 cause cleidocranial dysplasia. Cell. May 30 1997;89(5):773-9.

12. Bae SC, Lee YH. Phosphorylation, acetylation and ubiquitination: the molecular basis of RUNX regulation. Gene. Jan 17 2006;366(1):58-66.

13. Lee KS, Kim HJ, Li QL, Chi XZ, Ueta C, Komori T, et al. Runx2 is a common target of transforming growth factor beta1 and bone morphogenetic protein 2, and cooperation between Runx2 and Smad5 induces osteoblast-specific gene expression in the pluripotent mesenchymal precursor cell line C2C12. Molecular and cellular biology.

Dec 2000;20(23):8783-92.

14. Jeon EJ, Lee KY, Choi NS, Lee MH, Kim HN, Jin YH, et al. Bone morphogenetic protein-2 stimulates Runx2 acetylation. The Journal of biological chemistry. Jun 16 2006;281(24):16502-11.

15. Yoon WJ, Cho YD, Kim WJ, Bae HS, Islam R, Woo KM, et al. Prolyl isomerase Pin1-mediated conformational change and subnuclear focal accumulation of Runx2 are crucial for fibroblast growth factor 2 (FGF2)-induced osteoblast differentiation. The Journal of biological chemistry. Mar 28 2014;289(13):8828-38.

16. Park OJ, Kim HJ, Woo KM, Baek JH, Ryoo HM. FGF2-activated ERK mitogen-activated protein kinase enhances Runx2 acetylation and stabilization. The Journal of biological chemistry. Feb 5 2010;285(6):3568-74.

17. Cooper SC, Flaitz CM, Johnston DA, Lee B, Hecht JT. A natural history of cleidocranial dysplasia. American journal of medical genetics. Nov 15 2001;104(1):1-6.

18. Cohen MM, Jr. The new bone biology: pathologic, molecular, and clinical correlates. American journal of medical genetics Part A. Dec 01 2006;140(23):2646-706.

19. Rice DP. Craniofacial anomalies: from development to molecular pathogenesis. Current molecular medicine. Nov 2005;5(7):699-722.

20. Mendoza-Londono R, Lee B. Cleidocranial Dysplasia. In: Pagon RA,

Adam MP, Ardinger HH, Wallace SE, Amemiya A, Bean LJH, et al., editors. GeneReviews(R). Seattle (WA)1993.

21. Strahl BD, Allis CD. The language of covalent histone modifications. Nature. Jan 06 2000;403(6765):41-5.

22. Ito K, P JB, I MA. Histone acetylation and deacetylation. Methods in molecular medicine. 2000;44:309-19.

23. Wade PA. Transcriptional control at regulatory checkpoints by histone deacetylases: molecular connections between cancer and chromatin. Human molecular genetics. Apr 2001;10(7):693-8.

24. Bradley EW, Carpio LR, van Wijnen AJ, McGee-Lawrence ME, Westendorf JJ. Histone Deacetylases in Bone Development and Skeletal Disorders. Physiological reviews. Oct 2015;95(4):1359-81.

25. McGee-Lawrence ME, Westendorf JJ. Histone deacetylases in skeletal development and bone mass maintenance. Gene. Mar 15 2011;474(1-2):1-11.

26. Richon VM, Sandhoff TW, Rifkind RA, Marks PA. Histone deacetylase inhibitor selectively induces p21WAF1 expression and gene-associated histone acetylation. Proceedings of the National Academy of Sciences of the United States of America. Aug 29 2000;97(18):10014-9.

27. Kim HN, Lee JH, Bae SC, Ryoo HM, Kim HH, Ha H, et al. Histone deacetylase inhibitor MS-275 stimulates bone formation in part by enhancing Dhx36-mediated TNAP transcription. Journal of bone and

mineral research : the official journal of the American Society for Bone and Mineral Research. Sep 2011;26(9):2161-73.

28. Schroeder TM, Westendorf JJ. Histone deacetylase inhibitors promote osteoblast maturation. Journal of bone and mineral research : the official journal of the American Society for Bone and Mineral Research. Dec 2005;20(12):2254-63.

29. Cho YD, Yoon WJ, Woo KM, Baek JH, Park JC, Ryoo HM. The canonical BMP signaling pathway plays a crucial part in stimulation of dentin sialophosphoprotein expression by BMP-2. The Journal of biological chemistry. Nov 19 2010;285(47):36369-76.

30. Bae HS, Yoon WJ, Cho YD, Islam R, Shin HR, Kim BS, et al. An HDAC Inhibitor, Entinostat/MS-275, Partially Prevents Delayed Cranial Suture Closure in Heterozygous Runx2 Null Mice. Journal of bone and mineral research : the official journal of the American Society for Bone and Mineral Research. Jan 04 2017.

31. Kim HJ, Kim JH, Bae SC, Choi JY, Kim HJ, Ryoo HM. The protein kinase C pathway plays a central role in the fibroblast growth factor-stimulated expression and transactivation activity of Runx2. The Journal of biological chemistry. Jan 3 2003;278(1):319-26.

32. Komori T, Yagi H, Nomura S, Yamaguchi A, Sasaki K, Deguchi K, et al. Targeted disruption of Cbfa1 results in a complete lack of bone formation owing to maturational arrest of osteoblasts. Cell. May 30 1997;89(5):755-

64.

33. Bolger AM, Lohse M, Usadel B. Trimmomatic: a flexible trimmer for Illumina sequence data. Bioinformatics. Aug 1 2014;30(15):2114-20.

34. Kim D, Pertea G, Trapnell C, Pimentel H, Kelley R, Salzberg SL. TopHat2: accurate alignment of transcriptomes in the presence of insertions, deletions and gene fusions. Genome biology. 2013;14(4):R36.

35. Li H, Handsaker B, Wysoker A, Fennell T, Ruan J, Homer N, et al. The Sequence Alignment/Map format and SAMtools. Bioinformatics. Aug 15 2009;25(16):2078-9.

36. Anders S, Pyl PT, Huber W. HTSeq--a Python framework to work with high-throughput sequencing data. Bioinformatics. Jan 15 2015;31(2):166-9.

37. Young DW, Hassan MQ, Pratap J, Galindo M, Zaidi SK, Lee SH, et al. Mitotic occupancy and lineage-specific transcriptional control of rRNA genes by Runx2. Nature. Jan 25 2007;445(7126):442-6.

38. Ducy P, Zhang R, Geoffroy V, Ridall AL, Karsenty G. Osf2/Cbfa1: a transcriptional activator of osteoblast differentiation. Cell. May 30 1997;89(5):747-54.

39. Lou Y, Javed A, Hussain S, Colby J, Frederick D, Pratap J, et al. A Runx2 threshold for the cleidocranial dysplasia phenotype. Human molecular genetics. Feb 1 2009;18(3):556-68.

40. Kim HN, Lee JH, Jin WJ, Ko S, Jung K, Ha H, et al. MS-275, a benzamide histone deacetylase inhibitor, prevents osteoclastogenesis by down-

regulating c-Fos expression and suppresses bone loss in mice. European journal of pharmacology. Sep 15 2012;691(1-3):69-76.

41. Rot-Nikcevic I, Downing KJ, Hall BK, Kablar B. Development of the mouse mandibles and clavicles in the absence of skeletal myogenesis. Histology and histopathology. Jan 2007;22(1):51-60.

42. Kim HJ, Bae SC. Histone deacetylase inhibitors: molecular mechanisms of action and clinical trials as anti-cancer drugs. American journal of translational research. Feb 2011;3(2):166-79.

43. Gronroos E, Hellman U, Heldin CH, Ericsson J. Control of Smad7 stability by competition between acetylation and ubiquitination. Molecular cell. Sep 2002;10(3):483-93.

44. Geoffroy V, Ducy P, Karsenty G. A PEBP2 alpha/AML-1-related factor increases osteocalcin promoter activity through its binding to an osteoblast-specific cis-acting element. The Journal of biological chemistry. Dec 29 1995;270(52):30973-9.

45. Franci G, Casalino L, Petraglia F, Miceli M, Menafra R, Radic B, et al. The class I-specific HDAC inhibitor MS-275 modulates the differentiation potential of mouse embryonic stem cells. Biology open. 2013;2(10):1070-7.

46. Park MH, Shin HI, Choi JY, Nam SH, Kim YJ, Kim HJ, et al. Differential expression patterns of Runx2 isoforms in cranial suture morphogenesis. Journal of bone and mineral research : the official journal of the American Society for Bone and Mineral Research. May 2001;16(5):885-92.

47. Cho YD, Bae HS, Lee DS, Yoon WJ, Woo KM, Baek JH, et al. Epigenetic Priming Confers Direct Cell Trans-Differentiation from Adipocyte to Osteoblast in a Transgene-Free State. Journal of cellular physiology. Sep 3 2015.

48. Zhang YX, Sun HL, Liang H, Li K, Fan QM, Zhao QH. Dynamic and distinct histone modifications of osteogenic genes during osteogenic differentiation. Journal of biochemistry. Dec 2015;158(6):445-57.

49. Moon C, Kim SH, Park KS, Choi BK, Lee HS, Park JB, et al. Use of epigenetic modification to induce FOXP3 expression in naive T cells. Transplantation proceedings. Jun 2009;41(5):1848-54.

50. Cedar H, Bergman Y. Linking DNA methylation and histone modification: patterns and paradigms. Nature reviews Genetics. May 2009;10(5):295-304.

51. Dudakovic A, Camilleri ET, Xu F, Riester SM, McGee-Lawrence ME, Bradley EW, et al. Epigenetic Control of Skeletal Development by the Histone Methyltransferase Ezh2. The Journal of biological chemistry. Nov 13 2015;290(46):27604-17.

52. Schwarz D, Varum S, Zemke M, Scholer A, Baggiolini A, Draganova K, et al. Ezh2 is required for neural crest-derived cartilage and bone formation. Development. Feb 2014;141(4):867-77.

53. Bird A. DNA methylation patterns and epigenetic memory. Genes & development. Jan 1 2002;16(1):6-21.

54. Cho YD, Yoon WJ, Kim WJ, Woo KM, Baek JH, Lee G, et al. Epigenetic modifications and canonical wingless/int-1 class (WNT) signaling enable trans-differentiation of nonosteogenic cells into osteoblasts. The Journal of biological chemistry. Jul 18 2014;289(29):20120-8.

55. Kim HJ, Lee MH, Park HS, Park MH, Lee SW, Kim SY, et al. Erk pathway and activator protein 1 play crucial roles in FGF2-stimulated premature cranial suture closure. Developmental dynamics : an official publication of the American Association of Anatomists. Jul 2003;227(3):335-46.

56. Ali SA, Dobson JR, Lian JB, Stein JL, van Wijnen AJ, Zaidi SK, et al. A RUNX2-HDAC1 co-repressor complex regulates rRNA gene expression by modulating UBF acetylation. Journal of cell science. Jun 1 2012;125(Pt 11):2732-9.

57. Mirando AJ, Maruyama T, Fu J, Yu HM, Hsu W. beta-catenin/cyclin D1 mediated development of suture mesenchyme in calvarial morphogenesis. BMC developmental biology. 2010;10:116.

58. Behr B, Longaker MT, Quarto N. Absence of endochondral ossification and craniosynostosis in posterior frontal cranial sutures of Axin2(-/-) mice. PloS one. 2013;8(8):e70240.

59. Zhang X, Cowan CM, Jiang X, Soo C, Miao S, Carpenter D, et al. Nell-1 induces acrania-like cranioskeletal deformities during mouse embryonic development. Laboratory investigation; a journal of technical methods and pathology. Jul 2006;86(7):633-44.

60. Kumar R, Madewell JE, Swischuk LE, Lindell MM, David R. The clavicle: normal and abnormal. Radiographics : a review publication of the Radiological Society of North America, Inc. Jul 1989;9(4):677-706.

61. Arzenani MK, Zade AE, Ming Y, Vijverberg SJ, Zhang Z, Khan Z, et al. Genomic DNA hypomethylation by histone deacetylase inhibition implicates DNMT1 nuclear dynamics. Molecular and cellular biology. Oct 2011;31(19):4119-28.

62. Jensen ED, Nair AK, Westendorf JJ. Histone deacetylase co-repressor complex control of Runx2 and bone formation. Critical reviews in eukaryotic gene expression. 2007;17(3):187-96.

63. Gao X, Ma W, Nie J, Zhang C, Zhang J, Yao G, et al. A G-quadruplex DNA structure resolvase, RHAU, is essential for spermatogonia differentiation. Cell death & disease. 2015;6:e1610.

64. Dalgard CL, Van Quill KR, O'Brien JM. Evaluation of the in vitro and in vivo antitumor activity of histone deacetylase inhibitors for the therapy of retinoblastoma. Clinical cancer research : an official journal of the American Association for Cancer Research. May 15 2008;14(10):3113-23.

65. Menegola E, Di Renzo F, Broccia ML, Prudenziati M, Minucci S, Massa V, et al. Inhibition of histone deacetylase activity on specific embryonic tissues as a new mechanism for teratogenicity. Birth defects research Part B, Developmental and reproductive toxicology. Oct 2005;74(5):392-8.

66. Sengle G, Carlberg V, Tufa SF, Charbonneau NL, Smaldone S, Carlson EJ,

et al. Abnormal Activation of BMP Signaling Causes Myopathy in Fbn2 Null Mice. PLoS genetics. Jun 2015;11(6):e1005340.

67. Nistala H, Lee-Arteaga S, Smaldone S, Siciliano G, Carta L, Ono RN, et al. Fibrillin-1 and -2 differentially modulate endogenous TGF-beta and BMP bioavailability during bone formation. The Journal of cell biology. Sep 20 2010;190(6):1107-21.

68. James MJ, Jarvinen E, Wang XP, Thesleff I. Different roles of Runx2 during early neural crest-derived bone and tooth development. Journal of bone and mineral research : the official journal of the American Society for Bone and Mineral Research. Jul 2006;21(7):1034-44.

69. Wei S, Dai XM, Stanley ER. Transgenic expression of CSF-1 in CSF-1 receptor-expressing cells leads to macrophage activation, osteoporosis, and early death. Journal of leukocyte biology. Dec 2006;80(6):1445-53.

국문초록

Runx2$^{+/-}$ 두개쇄골이형성증 마우스에서 히스톤 탈아세틸화 효소 억제에 의한 뼈 이상 회복 기전 연구

서울대학교 대학원 치의과학과 분자유전학전공
(지도교수 류 현 모)
배 한 솔

Runx2/Cbfa1/AML3는 초기 골 분화 과정에서 핵심적인 역할을 하는 전사인자이다. *Runx2* 유전자의 전사나 단백질의 합성후수식 조절 기전에 저해되어 비정상적인 발현이 일어날 경우, 여러 골 질환을 야기하는 것으로 보고되어 있다. 본 연구에서는 두개쇄골이형성증 (Cleidocranial dysplasia; 이하 CCD)이라는 질환에 주목하여 약물을 처리하였을 때 증상 회복 여부를 분자생물학적 측면과 더불어 후성유전학 측면에서 확인하고 검증하였다.

CCD 는 상염색체 우성 유전질환으로, *RUNX2* 유전자의 반수체부족성에 의해 발병하는 것으로 알려져 있다. 대부분의 CCD 환자들의 주요 증상은 부진한 골격 발달로 인하여, 쇄골이 정상적으로 형성되지 않은 양상을 보이거나 두개골이 완전히 유합되지 않아

정상인보다 큰 천문을 가진다는 것이다. 현재까지 골 발달과 골다공증 등의 분야에서 RUNX2 에 대해 많은 연구가 이루어졌지만 아직까지 CCD 증상을 치료할 수 있는 약물요법은 개발되지 않은 실정이다. 최근 보고된 연구에 따르면 동물모델에서 CCD 표현형을 나타내는 데에는 *Runx2* mRNA 발현임계치가 존재한다고 한다. 우리는 이 연구 결과에 기반을 두어, 약물을 처리하여 정상적으로 기능하는 Runx2 의 양을 어느 수준까지 향상시킨다면 환자들의 CCD 증상을 완화할 수 있을 것이라 가설을 세우고 기존 연구에서 Runx2 의 발현 및 활성을 높여주는 것으로 규명한 약물, MS-275 (제 1 형 히스톤 탈아세틸화 효소 억제제)를 후보 약물로 선정하였다. 본 논문에서는 MS-275 를 동물모델 및 세포 모델에 처리하여 우리의 가설을 검증한 내용을 다루고 있으며 이를 통해 CCD 질환 치료제 개발의 기반을 마련하고자 하였다.

CCD 표현형을 나타내는 *Runx2*$^{+/-}$ 마우스의 태아에 MS-275 를 투약하였을 때 두개골의 유합 양상을 포함한 여러 골 기형이 정상 형질에 가깝게 회복되는 것을 확인 한 바, 이를 시작으로 실험적 검증을 통해 MS-275의 CCD 표현형 마우스에 대한 약물 효과는 다음 두 기전에 의하여 나타나는 것으로 설명할 수 있었다. (1) Runx2 단백질을 합성후수식 조절 (단백질 아세틸화)을 통해 안정화시켜 전사인자로써의 역할을 활성화시킨다. (2) 후성유전학적 조절을 통해 Runx2를 포함한 타

골 마커 유전자들의 발현을 증가시킨다. 또한, MS-275는 조골세포의 증식을 촉진한다는 것을 동물 조직과 세포 수준에서 규명하였다. 이는 CCD 환자에서 골격 형성이 부진하게 이루어지는 증상이 골전구세포들의 증식능 결함과 긴밀한 연관성이 있음을 시사한다.

이후 RNA 염기서열 분석을 통해 약물을 처리한 조직 및 세포에서 *Runx2* 반수체부족성 유전형이 되었을 때 발현이 증가하는 유전자 군과 감소하는 유전자 군으로 분류하여 각각의 유전자 군이 관여하고 있는 생물학적 기전을 생물정보학적으로 분석함으로써 *Runx2* 유전자 결핍에 의한 병인학적 현상을 유전자 수준에서 확인하였다. 한편으로는, MS-275를 처리하였을 때 발현양상이 정상형질 수준으로 되돌아가는 유전자 군을 확인함으로써 MS-275의 약리학적 효과를 확인할 수 있었으며, 이들이 관여하는 생물학적 기전이 대부분이 세포의 증식, 조골세포의 분화, 그리고 골격의 형성 및 유지에 관여하고 있음을 확인하고 앞서 수행한 *in vivo* 및 *in vitro* 연구와 상응하는 결론을 얻을 수 있었다.

본 논문에서는 MS-275라는 히스톤 탈아세틸화 효소 억제제가 Runx2 단백질을 안정화시키고 그와 동시에 *Runx2* 유전자 전사 및 골 형성 관련 유전자의 발현을 활성화시킴으로써 세포의 증식 및 조골세포 분화를 촉진하여 궁극적으로 CCD의 뼈 이상 회복 효과를 야기하였음을 보였다. 이 연구 결과는 약물치료법이 전무했던 CCD 질환에 대한 치료

제 개발 가능성을 열었다는 것과 MS-275에 의한 골전구세포 분화기전을 실험적·정보학적으로 규명하였다는데 의의가 있다.

Keywords : 두개쇄골이형성증, MS-275, 히스톤 탈아세틸화효소 억제제, Runx2 전사인자, 조골세포 분화, 골 형성
Student Number : 2011-22042